INVESTIGATION OF NATURAL RADIOACTIVITY LEVELS IN CONSTRUCTION ROCKS FROM SELECTED QUARRIES IN KERICHO COUNTY, KENYA USING GAMMA-RAY SPECTROMETRY

BETTY CHEPNGETICH

A THESIS SUBMITTED IN PARTIAL FULFILLMENT OF THE REQUIREMENTS FOR THE CONFERMENT OF THE DEGREE OF MASTER OF SCIENCE IN PHYSICS OF THE UNIVERSITY OF KABIANGA

UNIVERSITY OF KABIANGA

OCTOBER, 2024

DECLARATION AND APPROVAL

Declaration

This thesis is my original work and has not been submitted for the conferment of a degree or award of a diploma in this or any other institution.

Signature ……... Date ……

Chepngetich Betty

PGC/PHY/005/19

Approval

This thesis has been submitted with our approval as University Supervisors.

Signature…… Date……...

Dr. Fred Wekesa Masinde

Department of Mathematics, Actuarial, and Physical Sciences.

University of Kabianga.

Signature …… Date……

Dr. Enoch K Rotich Kipnoo

Department of Mathematics, Actuarial, and Physical Sciences.

University of Kabianga.

COPYRIGHT

ABSTRACT

The occurrence of naturally-occurring radionuclides, including Thorium-232, Uranium-238, and Potassium-40, in various environmental matrices such as soil, water, rocks, and food, is the primary cause of exposure to ionizing radiation. Radionuclides possess the capability to induce deleterious effects on human health through inhalation, ingestion or crops consumption, leading to detrimental impacts on living cells or DNA of the body. Higher radiation doses cause mutagenesis, which results in lung cancer, pediatric leukemia, kidney damage and death. Through the use of Gamma-ray Spectrometric analysis, this study investigated the natural activity concentration levels of Potassium-40, Thorium-232, and Uranium-238 in construction rocks from the 15 selected quarries in the County of Kericho, Kenya. Based on the geological distribution of the rocks used in building, quarries from each sub-county were selected. To improve the representation and the quality of the data, two samples were taken from each quarry. From sample collection through preparation and measurement, IAEA protocols were followed. In order to attain secular equilibrium between Radium-226 and Thorium-232, samples were collected, crushed, oven dried (105 °C), weighed, and put in airtight containers and were then preserved for four weeks. The determination of radiological parameters, including specific activity concentration, radium equivalent, annual effective dose rate, absorbed dose rate, external hazard index, internal hazard index, and activity utilization index, was done to determine the extent of radiation exposure to various groups of people who were constantly in contact with rock fragments, such as miners, transporters, masons, residents of homes constructed from these rocks, and even the general public. ^{232}Th, ^{238}U, and ^{40}K had average activity concentrations of 101± 5.08 Bq/kg, 56± 2.81 Bq/kg, and 1100 ±55.03 Bq/kg respectively and varied from 41± 2.07 to 138± 6.91 Bq/kg, 26 ±1.34 to 116 ±5.80 Bq/kg and 256±12.82 to 1919 ±95.99 Bq/kg respectively. The mean activity concentrations of ^{238}U, ^{232}Th, and ^{40}K were more than the global average values of 50 Bq/kg, 50 Bq/kg and 500 Bq/kg respectively. The Absorbed Daose Rate was greater than the global recommended value of 60 nGy/h but lower than the permissible threshold value of 1500 nGy/h, ranging from 83± 4.16 nGy/h to 152± 7.60 nGy/h with an average value of 138 ±6.94 nGy/h. The mean effective dose rates for indoor and outdoor environments were 0.6 ±0.03 mSv/y and 0.1±0 mSv/y respectively and were below the 1 mSv/y global recommendation. The mean activity utilization, internal hazard, and external hazard indices were 2.1±0.1, 0.9±0.04 and 0.8±0.04 mSv/y respectively. The average Radium equivalent value of 285 ±14.28 Bq/kg, which was below the permissible limit of 370 Bq/kg and ranged from 165 ±8.25 Bq/kg to 309 ±15.47 Bq/kg, indicated that the excavated rocks for construction from the chosen quarries in Kericho county pose negligible health risks to those who are in constant contact with the rock fragments and the general public.

DEDICATION

To my dear daughters Nicole Cherono Mutai, Hazel Chepkemoi Mutai and Imani Cheptoo Mutai, my dear son Shawn Toroitich Sitonik; my dear husband Cosmas Mutai, my dear late father David Sang, my dear mother Grace Sang, my sisters (Janeth Soy, Daisy Sang, Flossy Kemei, twin Betsy Chepngeno) and brothers (Evans Mutai, Aaron Mutai, Ambrose Mutai).

ACKNOWLEDGEMENT

I would want to offer my gratitude to the All-Powerful God for all of the benefits, mercies and the gift of life that He has bestowed upon me.

I would like to extend my profound gratitude to both of my supervisors , Dr. Fred Wekesa Masinde and Dr. Enoch K. Rotich Kipnoo, as well as the whole Mathematics, Actuarial, and Physical Sciences Department at the University of Kabianga, for their support and advice. Their expertise in radiometric analysis has been of considerable use to me in my studies, and I am grateful for that.

In addition, I would like to express my gratitude to the Department of Physical Sciences at South Eastern Kenya University (SEKU) for their support in the provision of the laboratory facilities. In particular, I would like to express my appreciation for Mr. Wanyama Conrad's expertise in the technical aspect s of the NaI(Tl) gamma-ray detector, which I used with his assistance.

I would like to express my gratitude to the Teachers' Service Commission for granting me study leave which enabled me to finish my coursework in a timely manner. I would also want to express my gratitude to the staff and students of Kaplong Boys High School and Kiptaragon Secondary School for their assistance and encouragement over the course of my study.

During the time that I was at school, I was supported financially, morally and spiritually by a number of people, including my late father David Sang, my father in-law Ezekiel Yegon, my mother Grace Sang, my mother in-law Lily Yegon, my sisters, my brothers, my husband Cosmas Mutai, my brothers in-law, my sister in-law and the students in my class and I am grateful to them. My special appreciations goes to my sister Daisy, my brother in-law Leonard Mutai and my nieces Faith and Abigael for their support.

TABLE OF CONTENTS

LIST OF FIGURES

LIST OF TABLES

LIST OF ABBREVIATIONS AND ACRONYMS

AC	Activity Concentration
AEDE	Annual Effective Dose Equivalent
AEDR	Annual Effective Dose Rate
AGDE	Annual Gonadal Dose Equivalent
ADR	Absorbed Dose Rate
DNA	Deoxyribonucleic Acid
ECLR	Excess Lifetime Cancer Risk
EPA	Environment Protection Agency (USA)
GPS	Global Positioning System
HBRA	High Background Radiation Area
HPGe	High-Purity Germanium- Detector
IAEA	International Atomic Energy Association
ICRP	International Commission on Radiation Protection
IEBC	Independent Electoral and Boundaries Commission
KCP	Kenya Cancer Policy
KPHC	Kenya Population and Housing Census
KRPB	Kenya Radiation Protection Board
NaI (TI)	Thallium-activated Sodium Iodide detector
NBRA	Normal Background Radiation Area

NORM	Naturally Occurring Radioactive Materials
NRPB	National Radiation Protection Board
RLI	Representative Level Index
TENORM	Technologically Enhanced Naturally Occurring Radioactive Materials
UNSCEAR	United Nations Committee on Effects of Atomic Radiations
WHO	World Health Organisation
XRF	X-ray fluorescence

LIST OF SYMBOLS

$Bqkg^{-1}$	Becquerel per kilogram
E	Photon Energy
E_a	Atoms Kinetic Energy
E_b	Binding Energy
E_e	Electrons Kinetic Energy
E_p	Energy of Positron
E´	Energy of Scattered Gamma Ray
H_{ex}	External Hazard Index
H_{in}	Internal Hazard Index
H_T	Equivalent Dose
I_{yr}	Activity Utilization Index
$mSvy^{-1}$	milli Sievert per year
$nGyh^{-1}$	nano Gray per hour
$SvGy^{-1}$	Sievert Gray per year
Q_F	Quality (Modifying) factor
Z	Atomic number
τ	probability of photoelectric occurrence
μSvy^{-1}	micro Sievert per year

CHAPTER ONE

INTRODUCTION

1.1 Overview

This chapter provides an overview of the research background, sources of radiation, research objectives, justification, research significance, and study scope.

1.2 Background of the study

Individuals are subjected to ionising background radiation which may originate from primordial radionuclides like Thorium-232 (^{232}Th), Uranium-238 (^{238}U), as well as their decay products and Potassium-40 (^{40}K), either through internal or external exposure. There are many different sources of radionuclides in the environment, including the soil, the water, the rocks, and even the food. Inhaling polluted air or ingesting tainted food or water are two of the ways that these chemicals may make their way into human systems.

Ionising radiations commonly referred to as radioactivity according to Rasmussen & Ellis (2023), are generated through the process of an unstable nucleus decaying into a stable state. The process of extracting minerals involves collecting rocks, which may put workers at risk of being exposed to ionising radiation. This radiation comes from the natural radioisotopes that are present in the rocks themselves, and it can cause cancer in humans. Isotopes ^{238}U and ^{232}Th, as well as their respective decay products and isotope ^{40}K are all observable inside the geological layer of the crust of the earth, which includes soil, water and rocks.

Human beings are subjected to ionising radiation from isotopes that may be found in both indoor and outdoor environments (Kebwaro et al., 2011). Radiation may be

emitted by construction materials including soil, rocks and the foundation of the structure, which can lead to indoor exposure. If the radiation level is high enough, the possible presence of primordial radionuclides in construction rocks has the potential to endanger a wide variety of people. These individuals include miners, masons, transporters, nearby residents to quarries, and occupants of structures built from these rocks. This is the case only if the radiation level is high enough to exceed the acceptable thresholds. In both indoor and outdoor environments, ICRP , (2005) recommends keeping the annual effective dose rate (AEDR) at 1 $mSvy^{-1}$ and the average radium equivalent (Ra_{eq}) below 370 $Bqkg^{-1}$. Table 1.1 presents the recommended thresholds for radiological parameters.

Table 1.1: Recommended Limits of the Radiological Parameters

Radiological parameter	**Recommended values**
AC of U-238 and Th-232	<50Bq/kg
AC of K-40	<500Bq/kg
Radium equivalent	<370Bq/kg
Absorbed dose rate	<60nGy/h
Annual effective dose rate	<1mSv/y
Radiation hazard indices	<1mSv/y

Source: UNSCEAR, (2000)

The degree of natural radioactivity exposure caused by radiation is dependent on geological factors, leading to fluctuating levels of radioactivity in rocks. Various construction materials, including but not limited to soil and rocks, possess intrinsic primordial radioisotopes that pertain to the ^{238}U and ^{232}Th series (UNSCEAR, 2000). The decay series/chain of ^{238}U and ^{232}Th is presented in Figure A7 (Appendix VI). The existence of Potassium-40 is a contributing factor to the total radiation exposure

encountered by individuals who dwell in residences built with rock materials. The dwellings in question emit gamma radiation from their walls, ceilings and floors due to the absorption of radon, thorium, and their respective offspring.

Tzortzis et al., (2004) found that sedimentary rocks, metamorphic rocks and igneous rocks make up the majority of the Earth's crust. According to UNSCEAR, (2000), igneous rocks contain much more ^{40}K, ^{238}U, and ^{232}Th than other rock types. These findings were based on observations made via the use of radiometric survey records. In addition to the inhalation of radon gases and dust particles, one of the primary ways in which radionuclides may enter the human body is via the consumption of foods derived from plants, notably K-40. According to Singh et al., (2005) there is a considerable risk associated with the eating of food by humans that is cultivated in areas where there is a possibility of increased levels of naturally occurring radionuclides.

1.2.1 Sources of radiations

According to Faanu et al., (2016), radiation emanates primarily from naturally occurring radioactive materials (NORM) and technologically enhanced naturally occurring radioactive materials (TENORM). The NORM family of compounds which encompasses radium, potassium, uranium and thorium as well as their corresponding decay products, are examples of unadulterated molecules that have not been subject to any human manipulation. Background radiation is a phenomenon brought on by the influx of radiation from high-energy particles such as cosmic radiation emitted by the sun and stars, the presence of radionuclides like ^{238}U and ^{232}Th as well as their decay products and naturally occurring ^{40}K that is present on the earth's surface. This exposure to radioactive substances can occur either internally or externally and has been documented in studies such as that conducted by Mulwa et al., (2013).

Potassium-40 and Carbon-14 are known to exist in various environmental sources such as food, soil and water, thereby leading to the generation of endogenous radiations within the human body (Faanu et al., 2016). The TENORM are exposed naturally occurring radioactive materials due to industrial processes, for example, the medical facilities (medical radiotherapy and X-rays) and nuclear industry (nuclear weapons and power plants tests and accidents, i.e. Chernobyl nuclear power plant in Ukraine).

Humans are exposed to about 85% of NORM radiations and about 15% of TENORM radiations. Nuclear industry and medicine, which are TENORM contribute 1% and 14% respectively, whereas Radon, rocks and soil, drinking water and food, and cosmic rays, which are NORM contributes 42%, 18%, 11% and 14% respectively, as shown in Figure 1.1. (UNSCEAR, 2000).

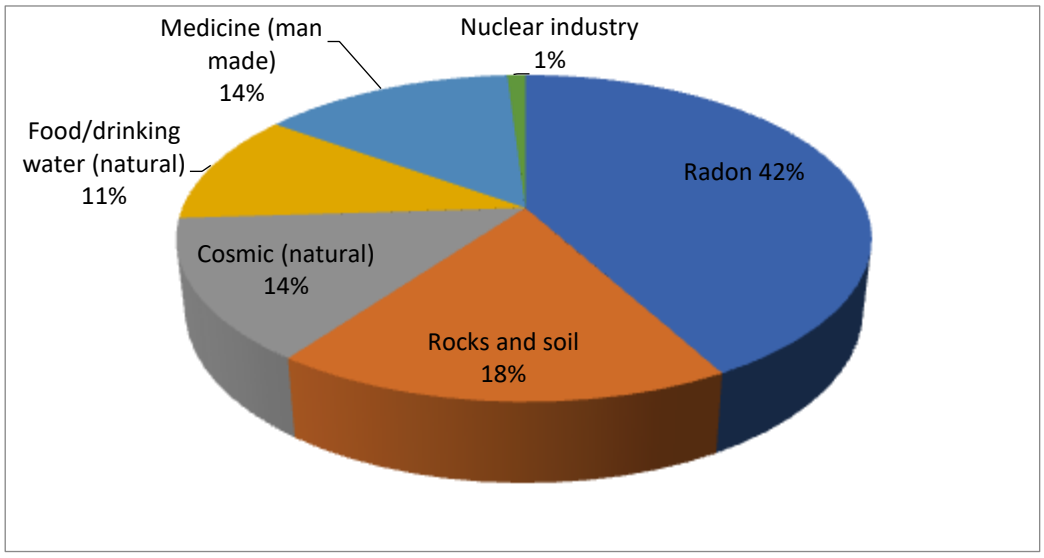

Figure 1.1: Percentage abundance due to NORM and TENORM sources (UNSCEAR, 2000).

1.2.2 Effects of radiations on living matter (life)

Ionizing radiations damage the internal functioning of organs or tissues if the matter is subjected to prolonged exposure. These radiations damage the DNA causing cellular

deaths, mutagenesis (modification of genetic information by radiations or chemicals) and genetic transmutation. Inhalation of radon gases and large concentrations of uranium causes lung cancer, whereas ingestion of radon causes kidney damage (UNSCEAR, 2000). When radon and its offspring (polonium-218, polonium-214 and lead-214) decay in the air, they emit radiations that cause DNA damage in body cells and when DNA mutations are inherited, they may cause cancer. Additionally, radon exposure causes leukemia and birth abnormalities in children. The International Agency for the Study of Cancer (IARC) has identified radon and its derivatives as carcinogens (UNSCEAR, 2000). According to the EPA, radon is categorized as the second largest cause of lung cancer while smoking cigarettes is the first cause (KCP, 2019). External radiations (ultraviolet) from Cosmogenic materials cause sunburns (damaging skin). If the ultraviolet exposure is prolonged, it causes skin cancer due to the mutation of genetic information in skin cells. Even though prolonged exposures to these radiations are harmful to matter, they are useful in the medical industry for radiation therapy to mutate and kill cancer cells under high control (Rich, 2007).

1.3 Statement of the problem

Cancer cases and mortalities has been on a higher rise across the country. According to the Kenya Cancer Policy (KCP), there has been a rise in cancer incidence and deaths which rose from 37000 and 28500 in 2012 to 47887 and 32987 in 2018, respectively. Kericho County recorded an increase in cancer cases as per the statistics from the three major public health facilities in the county over a period of four years. Cancer cases recorded by Kericho County Referral Hospital in the year 2018, 2019, 2020 and 2021 were 35, 39, 41 and 49 respectively. Kapkatet County Hospital recorded 32, 30, 35 and 41 cancer cases in the year 2018, 2019, 2020 and 2021 respectively, whereas Londiani County Hospital recorded 22, 33, 32 and 35 cancer

cases In the year 2018, 2019, 2020 and 2021 respectively . This can be attributed to the radiations from primordial radioisotopes found in the rocks excavated from the county. Excavating rocks used to construct commercial and domestic houses in Kericho County and neighbouring counties is striving economic activity. Miners, transporters, masons, populace around the quarries and inhabitants of the houses built from these construction rocks may be exposed to radiations from ^{238}U, ^{232}Th, their decay products and ^{40}K primordial radioisotopes found in these construction rocks due to constant interaction with the rock fragments and inhalation of radon gases if the radiation levels are beyond permissible levels. This leads to the damaging of living cells, causing lung cancer, kidney damage and even deaths. Despite the constant interaction of different categories of human beings with the rock fragments from the quarries in Kericho County, there is limited reported data and literature on the levels of radiations from the primordial radioisotopes as well as their decay products in these rocks. Radiation exposure must be kept below the world health organisation's recommended minimal levels since even shallow doses might cause cancer over a lengthy period. This research determined the levels of radiations in construction rocks that are excavated from selected quarries within Kericho County. It is possible that further technical breakthroughs and infrastructure development would increase the risks associated with radiation exposure.

1.4 Objective of the study

1.4.1 General objective

The main objective of this study was to investigate the natural radioactivity levels in construction rocks from selected quarries in Kericho County, Kenya using Gamma-ray Spectrometry.

1.4.2 Specific objectives

i) To determine the activity concentration of K-40, Th-232 and U-238 in the rock samples.

ii) To determine the radiological hazard indices (external and internal), utilization index and radium equivalent associated with K-40, Th-232 and U-238 in rock samples.

iii) To determine the absorbed dose rate and annual effective dose rates using the concentration of K-40, Th-232 and U-238 in rock samples.

1.5 Research questions

i) What are the activity concentrations of K-40, Th-232, and U-238 in the rock samples?

ii) What are the radiological hazard indices (external and internal), utilization index and radium equivalent associated K-40, Th-232, and U-238 in rock samples?

iii) What are the dose rates (absorbed and annual effective) based on the concentration of K-40, Th-232, and U-238 in rock samples?

1.6 Justification of the Study

Cancer cases and mortalities has been on a higher rise across the country. Kericho county has also reported rising cases and mortalities of cancer according to the statistics obtained from three major health facilities within the county. Lung cancer is caused by smoking of cigarette and ionizing radiations from primordial radionuclides which are found in rocks. The extraction of rocks utilized for construction purposes from diverse quarries situated in Kericho County serves as a means of livelihood for the local population residing in the surrounding regions. Residents of these areas depend majorly on selling the rocks used for construction to the residents of Kericho

County and beyond, boosting the economy of those areas and the county at large. The people in constant interaction with the rock fragments are miners (during the excavation process), masons (during the construction period), transporters, and inhabitants of commercial and domestic houses built from these construction rocks. The continuous interaction of diverse groups of inhabitants from Kericho County and its environs with rock fragments sourced from quarries poses a potential hazard of radiation exposure from primordial radionuclides that may surpass the acceptable threshold, if present in the construction rocks. In order to mitigate this potential hazard, this research investigation provides levels regarding the radiological parameters of rocks utilized in construction sourced from selected quarries located in Kericho County. The information about the levels of natural radioactivity of ^{40}K, ^{232}Th, and ^{238}U findings will assist the Kericho County Government, the National Government of Kenya, and other relevant bodies such as the KRPB, WHO and NRPB in determining the safety of the populace in the vicinity of these quarries and residents of houses constructed from these construction rocks within Kericho County and beyond.

1.7 Significance of the study

According to Kenya Cancer Policy (KCP), cancer cases and mortalities has been on a higher rise (KCP, 2019). Cause of the cancer related diseases has been attributed to radiations from radioisotopes like ^{238}U and ^{232}Th and ^{40}K that are present in rocks excavated for building (mineral mining). Their decay products and the single-occurrence ^{40}K might result in enhanced radiation exposure depending on the geological circumstances (UNSCEAR, 2000).

The individuals involved in mining, transportation, masonry, and inhabitation of dwellings constructed from such rocks, as well as the general public residing in the

vicinity of quarries, face potential risks associated with exposure to primordial radionuclide emissions that exceed permissible limits.

Limited literature and data on the levels of radiological parameters of the rocks excavated within Kericho County has been documented inspite of the rising cases of cancer.

It is on this basis that the findings and suggestions of this study hold their significance in offering knowledge and awareness on the safety of rocks for public use and relevant bodies.

1.8 The scope of the study

The goal of the study was to examine the levels of radioactive elements detected in the building stones sourced from the Kericho county. This investigation focused on examining the radiation levels of ^{238}U, ^{232}Th and ^{40}K, which possess half-lives of 4.5×10^{9} years, 1.4×10^{10} years, and 1.25×10^{9} years, respectively. The evaluation of radiation levels can provide an estimation of the radiological information and dose rate impact of primordial radionuclides, namely ^{238}U, ^{232}Th and ^{40}K. The study focuses on 15 quarries selected from the six sub-counties in Kericho County where two samples were collected from each quarry, making 30 samples.

CHAPTER TWO

LITERATURE REVIEW

2.1 Introduction

This chapter provides a discourse on the yearly effective doses, radiation hazard indices, and absorbed doses that have been assessed through the utilisation of the activities of the decay series of uranium, potassium, and thorium. The surveys conducted in various locations around the world, as well as in Kenya, are relevant to the subject matter of this study. The identified gap has been associated with corresponding recommendations for each radiological study, and the theoretical framework has been emphasized accordingly.

2.2 Empirical literature

2.2.1 Radiometric analysis globally

Human activities, such as waste disposal, frequently have negative impacts on the environment due to some waste materials displaying elevated levels of intrinsic radioactivity. Onjefu et al., (2021) examined the potential health hazards linked to the natural radioactivity emanating from the Okakarara municipal waste dumpsite situated in Namibia. The investigation employed gamma spectrometry analysis as a means of determining the activity concentrations of ^{226}Ra, ^{232}Th, and ^{40}K of 18 soil samples from the dumpsite. The investigation found that the average activity concentrations of ^{226}Ra, ^{232}Th and ^{40}K were 15.45±0.47 Bqkg^{-1}, 18.00±0.55 Bqkg^{-1} and 215.73±4.29 Bqkg^{-1} respectively. The mean value of Ra_{eq} obtained was 57.80±0.98 Bqkg^{-1} hence below the globally acknowledged threshold of 370 Bq.kg^{-1}. The study determined that the absorbed dose rate was 27.00±0.44 nGy.h^{-1} and the average annual effective dose equivalent (AEDE) value was 0.03 mSv.y^{-1}. The research findings indicate that the Annual Gonadal Dose Equivalent (AGDE) was

determined to be 190.89 $\mu Sv.y^{-1}$, which is lower than the global average level of 298 $\mu Sv.y^{-1}$. The study determined that the mean Representative Level Index (RLI) was 0.43 mSv/y and External Hazard Index (H_{ex}) was 0.16 mSv/y. The indices' values were found to be below one. The average ECLR was computed to be 1.16 x 10^{-4}. The measured quantity has registered a value that is below the internationally accepted limit level of 2.9 x 10^{-4}. This study concluded that the natural radioactivity emitted from Okakarara wasteland area did not present any noteworthy health hazards.

The study conducted by Khan et al., (2020) aimed to evaluate the plausible health hazards that may arise from the existing radioactive nuclides in the soil of North Waziristan, Pakistan, on the general public. The collected samples from the study area underwent analysis for radioactivity through utilization of an HPGe system that was appropriately shielded against background radiation. The investigation showed that the radioactivity concentration ranged from 42.6 to 106.3 Bq/kg for Ra-226, 4.0 to 93.8 Bq/kg for Th-232, 49.9 to 645.5 Bq/kg for K-40, and 2.6 to 8.33 Bq/kg for Cs-137. The study determined the mean values of the external and internal hazards indices, represented as H_{ex} and H_{in} respectively, to be 0.75 and 0.95 mSv/y. The investigation further found that the activity Radium equivalent of three distinct sites, specifically Datta Khel, Khaisur forest, and Jani Khel, to be 422.081 Bq/kg, 407.938 Bq/kg, and 379.213 Bq/kg, respectively. The mean absorbed dose rate was calculated to be 101 nGy/h, which consequently led to an annual effective dose rate of 0.15 mSv/y in outdoor settings. The study's results demonstrate a stronger positive correlation between radioactive isotopes and their associated radiological variables, with statistical significance at a level of $P \leq 0.01$. The findings validate that γ-radiation emission is primarily attributed to Ra-226 and Th-232. These authors discovered that certain regions in North Waziristan exhibit elevated levels of

radioactivity concentrations and corresponding radiometric parameters, surpassing the global average values. This suggests that inhabitants of these regions may face potential radiological hazards.

Mamuju in Indonesia has been linked to significant levels of radiation exposure because of its naturally occurring uranium concentration. Several mapping investigations by Syaeful et al., (2014) found a high NORM in the geological genesis of Adang volcano. Research on the natural radioactivity of volcanic and laterite rock samples in Mamuju was undertaken by Rosianna et al., (2020) where 30 rock samples were collected. X-ray fluorescence (XRF) was utilized to analyze laterite and volcanic rock samples for their constituent components. It was discovered that activity levels of ^{238}U and ^{232}Th radionuclides were greater than allowed by an HPGe detector. Between 539 and 128,699 $Bqkg^{-1}$ (an average of 22,882 ± 1602 $Bqkg^{-1}$), 471-288,639 $Bqkg^{-1}$ (an average of 33,549 ± 2348 $Bqkg^{-1}$), and 69-23,088 $Bqkg^{-1}$ (an average of 1909 ± 134 $Bqkg^{-1}$) are the activity concentrations of ^{238}U, ^{232}Th, and ^{40}K, respectively.

A study on the levels of radiation on basalt rocks in Wadi Khuda area in Eastern, Egypt was conducted where 21 samples were collected, measured and analysed using NaI(TI) gamma ray spectrometry. The rocks were found to have a Radium equivalent activity (Ra_{eq}) of 131.72 $Bqkg^{-1}$. Additionally, the Internal Hazard (H_{in}), External Hazard (H_{ex}), and Representative Level (RLI) indices were determined to be 0.5, 0.35, and 1.05, respectively. The Dose Rate (D), Indoor Annual Effective Radiation (AER), and Outdoor Annual Effective Radiation (AER) are reported as 65.585 $nGyh^{-1}$, 321.755 $nSvy^{-1}$, and 80.435 $nSvy^{-1}$ respectively. Gamma radiation was shown to have a lower Gonadal Dose Equivalent (AGDE) than the global average of 300 Svy^{-1}. The

extra cancer risk over the course of one's lifetime was estimated and was found to be greater than the global average of 2.9×10^{-4}. It is safe to conclude that there is minimal health danger to Wadi Khuda region people since the average findings from study were lower than the world's suggested values (As-Subahihi et al., 2019).

In a study on uranium favourability in North Eastern Nigeria, the Kerri-Kerri Formation in, upper Benue Trough was identified as a possible host for uranium minerals, hence the need to asses the level of natural gamma radiation from the rocks in the area. Laboratory γ-ray spectrometric analysis was carried out with a HPGe detector. Thirty six rock samples were collected from the study area from which nine composite samples were formed for the laboratory γ-ray analysis. The study determined the mean concentration levels of radionuclides ^{238}U, ^{232}Th and ^{40}K to be 26.9988 Bq/kg, 61.9131 Bq/kg, and 91.7042 Bq/kg, respectively and the average absorbed dose rate was 15.646 $nGyh^{-1}$, which falls below the universally recognized standard. Both the internal and the exterior hazard indices were determined to be much lower than the minimal acceptable level of 1. The study revealed that the mean radium equivalent (Ra_{eq}) value was below the hazardous threshold, indicating a significant decrease in potential risk. The researchers concluded that the rocks could be safely used for construction and building purposes (Bachama et al., 2017).

In a recent investigation conducted in southwest Uganda, it was found that the activity concentration levels present on mine tailings were significantly higher than the permissible limits. The study indicates that the effective dosages resulting from these mining activities varied between 0.34 mSv/y and 0.39 mSv/y. Furthermore, the research reported alarming values for radioactive isotopes, including concentrations of 238U ranging from 35.5 to 147.0 Bq/kg, 232Th ranging from 119.3 to 376.7 Bq/kg, and 40K exhibiting levels between 141.0 and 1658.5 Bq/kg. The absorbed dose rates

recorded at various sites, such as Kikagati Tin Mine, Butare Iron Ore Mine, and Mashonga Gold Mine, were found to be 181.2 ± 66.8 nGy/h, 167.2 ± 43.0 nGy/h, and 191.6 ± 29.6 nGy/h, respectively. These findings highlight a concerning public health risk, as the recorded values exceed acceptable limits, posing potential health hazards to the local population (Turyahabwa et al., 2016).

The researchers in Ghana conducted a study into the levels of natural radioactivity present in soil, rocks, and water through the use of direct-gamma spectrometry. The results of their study demonstrate that the average absorbed dose rate in the air was 0.08± 0.02 μGyh^{-1}, and the mean annual effective dose rate was 0.093±0.028 mSv/y. The investigation demonstrated that the specimens of soil, rocks and ore exhibited radioisotope levels of 65.1±2.2 $Bqkg^{-1}$, 71.8±2.2 $Bqkg^{-1}$, and 1168.3 $Bqkg^{-1}$ of ^{238}U, ^{232}Th and ^{40}K correspondingly. Furthermore, the mean radium equivalent activity concentration in the soil, rocks, and ore specimens was ascertained to be 257.8±62.4 $Bqkg^{-1}$. The investigation demonstrated a yearly delivery of 0.91±0.32 mSv, accompanied by an average external dose rate of 0.7±0.2 mSv/y and an average internal dose rate of 0.9±0.2 mSv/y. The analysis of the soils, rocks and ore revealed that the detected radiation levels were within the permissible limits, thus indicating that they are safe for human consumption (Faanu et al., 2016).

A radiological study was conducted to assess the levels of radionuclides in basalt rocks sourced from the Aden Governorate in South Yemen. This investigation utilized a sodium iodide (NaI(Tl)) detector, which is widely recognized for its effectiveness in measuring and analyzing gamma radiation. A total of 63 basalt rock samples were collected for this purpose. The primary focus of the study was to evaluate the levels of radioactivity within these rocks, specifically the radium equivalent activity, which is a

crucial metric in assessing radiological safety.The results of the study revealed that the average radium equivalent activity (Ra_{eq}) was measured at 237.01 $Bqkg^{-1}$. This figure is notably lower than the established permissible limit of 370 $Bqkg^{-1}$ set for safe exposure. Such a finding is significant, as it suggests that the basalt rocks from this region do not pose an immediate radiological hazard based on radium levels. In addition to Ra_{eq}, the study also calculated the average gamma dose rate absorbed, symbolized as D. The gamma dose rate was found to be 55 $nGyh^{-1}$, which provides insight into the amount of gamma radiation that individuals in the vicinity might be exposed to from the rocks. Understanding this dose rate is essential for evaluating potential health risks associated with gamma radiation exposure. The study further investigated the annual effective dose rates for both external and internal exposure. These dose rates were determined to be 0.11 $mSvy^{-1}$ for external exposure and 0.03 $mSvy^{-1}$ for internal exposure. These values are important for understanding the potential long-term health impacts of radiation exposure on the local population. To assess the safety levels of the basalt rocks more comprehensively, the researchers computed the external hazard index (H_{ex}) and the internal hazard index (H_{in}). The Hex was found to be 0.138, while the Hin was calculated at 0.154. These indices help in determining the potential risk associated with radioactive materials and are essential for regulatory assessments. Additionally, the index representing the level of representation, denoted as I_{yr}, was calculated to be 0.386. This index provides a further layer of understanding regarding the radiological profile of the basalt rocks and their potential impact on the environment and human health. The study noted that the values obtained for radium equivalent activity, gamma dose rates, and hazard indices were higher than the average global values. This discrepancy highlights the importance of localized studies in understanding the specific radiological

characteristics of materials in different geographic regions.In summary, the radiological study of basalt rocks from Aden Governorate provided critical insights into the levels of radionuclides present in these samples. The findings indicate that while the radium equivalent activity and gamma dose rates are below safety limits, the calculated indices suggest a need for ongoing monitoring and assessment. Understanding these levels is vital for ensuring public health and safety in areas where such geological materials are present. (Harb et al., 2014)

A comprehensive radioactivity survey of basalt rocks in the vicinity of Sidikan, Iraq, was conducted by researchers Ahmed & Hussein, (2011). The study aimed to assess the levels of radioactivity in the region's geological materials, focusing specifically on basalt rock samples known for their potential radiological significance. To carry out the analysis, the researchers collected a total of eight basalt rock samples. The measurement and analysis of these samples were performed using advanced detection equipment, namely a Planar High-Purity Germanium (HPGe) detector and a sodium iodide (NaI(TI)) detector. These detectors are widely utilized in the field of radiation measurement due to their precision and effectiveness in identifying and quantifying radioactive isotopes. The results of the survey indicated that the average radium equivalent activity, referred to as Raeq, was measured at 44.8 $Bqkg^{-1}$. This value is significantly lower than the globally recognized permissible limit of 370 $Bqkg^{-1}$, which is often used as a benchmark for assessing the safety of radioactive materials. The low level of radium equivalent found in the basalt rocks near Sidikan suggests that these materials pose little to no risk of radiological harm to individuals or the surrounding environment. In addition to determining the radium equivalent, the study also focused on calculating several important metrics related to radiation exposure. One key measurement was the average gamma dose rate, symbolized as D, which was

assessed in nanograys per hour ($nGyh^{-1}$). The findings revealed that the dose rate in this region was lower than the world average, indicating a relatively safe environment in terms of gamma radiation exposure. Similarly, the annual effective dose rates for both internal and external exposure were calculated and referred to as $AEDR_{in}$ and $AEDR_{out}$, respectively. These values were also found to be below the global averages of 0.11 $mSvy^{-1}$ for external exposure and 0.03 $mSvy^{-1}$ for internal exposure. The low measurements of D, $AEDR_{in}$, and $AEDR_{out}$ are significant because they suggest that the community living in proximity to these basalt rocks is not exposed to harmful amounts of radiation. Such findings are reassuring, particularly for residents and workers in the area, as prolonged exposure to elevated radiation levels can lead to adverse health effects. The implications of these findings extend beyond just the immediate community. By establishing that the radioactivity levels in the basalt rocks near Sidikan are well below global safety standards, the study contributes valuable data for regional environmental assessments and public health policies. This information can help guide future research and monitoring efforts to ensure that the radiological safety of geological materials remains a priority in Iraq and similar regions. In summary, the survey conducted by Ahmed and Hussein provides critical insights into the radioactivity levels of basalt rocks in Sidikan, Iraq. The findings indicate that the radium equivalent activity and gamma dose rates are significantly lower than globally accepted limits, thereby ensuring that the local community is not exposed to harmful radiation levels. The study underscores the importance of ongoing monitoring and research in understanding the radiological safety of geological formations in various regions (Ahmed & Hussein, 2011).

In a comprehensive study conducted by Uosif, (2011), gamma-ray spectrometry utilizing a sodium iodide (NaI(TI)) detector was employed to measure and evaluate a

total of 43 samples of construction materials sourced from Upper Egypt. The primary aim of this investigation was to assess the radioactivity levels present in these materials, which are crucial for ensuring safety in construction practices. The use of gamma-ray spectrometry is particularly valuable in this context, as it provides accurate measurements of various radionuclides, thus allowing for a thorough evaluation of the materials' radiological properties. The findings of the study indicated that the rates of absorbed dose in indoor environments varied between 0.19 to 0.51 $nGyh^{-1}$. This range highlights the differing levels of gamma radiation exposure that individuals might encounter in buildings constructed with these materials. Importantly, the annual effective doses, which represent the total radiation exposure over a year, ranged from 0.9 to 3.5 μSvy^{-1}. These values were found to be significantly lower than the established threshold limits set by international safety standards, indicating that the levels of radiation exposure associated with these construction materials are well within safe limits for human health. Additionally, the study focused on the activity concentrations of key radionuclides, specifically Thorium-232 (^{232}Th), Radium-226 (^{226}Ra), and Potassium-40 (^{40}K). The activity concentration values for these isotopes were measured across the samples, yielding results for 232Th ranging from 17 ± 1 to 115 ± 6 $Bqkg^{-1}$, for 226Ra from 17 ± 1 to 79 ± 4 $Bqkg^{-1}$, and for 40K from 95 ± 5 to 376 ± 19 $Bqkg^{-1}$. These findings are critical as they provide insight into the specific types of radiation that may be emitted from the construction materials. The recorded activity concentrations for all three radionuclides were notably below permissible levels, which further reinforces the safety of using these materials in construction. The conclusion drawn from this study is significant. Since the activity concentration values and absorbed dose rates were found to be below the permissible limits, the construction materials evaluated in Upper Egypt

were deemed safe for use in new buildings, pavements, and flooring. This recommendation is essential for ensuring that future construction projects do not inadvertently expose residents to harmful levels of radiation, thereby safeguarding public health. Moreover, this study contributes to a broader understanding of the radiological safety of construction materials, an important aspect of building regulations and safety standards. By providing reliable data on the radioactivity of materials commonly used in construction, it supports informed decision-making in the industry. In summary, Uosif's 2011 study effectively assessed the radioactivity levels in construction materials from Upper Egypt using gamma-ray spectrometry. The results indicated that absorbed dose rates and annual effective doses were within safe limits, while the activity concentrations of ^{232}Th, ^{226}Ra, and ^{40}K were below permissible levels. Consequently, these materials were recommended for use in various construction applications, ensuring that they meet safety standards and contribute to the health and well-being of the community. (Uosif, 2011).

Erasama Beach in India, known for its rich deposits of monazite, has garnered attention due to its elevated levels of radiation, categorizing it as a "high background radiation region." This classification is significant because it indicates that the area experiences higher than normal radiation levels, which can have implications for both environmental health and safety. To accurately measure and evaluate the radiation levels present in this unique environment, researchers utilized a High-Purity Germanium (HPGe) detector. This advanced detection technology is widely recognized for its sensitivity and precision in identifying various radionuclides, making it an ideal choice for analyzing bulk sand samples from the beach. The HPGe detector's capability allows for a comprehensive assessment of the radiological characteristics of the sand, which is essential for understanding the potential health

risks associated with prolonged exposure to radiation. The study revealed that the average activity concentrations of specific radionuclides present in the sand were significantly high. The measured values were 2825 ± 50 $Bqkg^{-1}$ for Thorium-232 (^{232}Th), 350 ± 20 $Bqkg^{-1}$ for Uranium-238 (^{238}U), and 180 ± 25 $Bqkg^{-1}$ for Potassium-40 (^{40}K). These concentrations indicate that the sand at Erasama Beach contains substantial levels of natural radioactivity, particularly from thorium, which is commonly found in monazite. Such high activity concentrations can contribute to the overall radiation exposure for individuals in the area, making it important to monitor and assess potential health implications. Further analysis of the external effective dose rates, which represent the annual radiation exposure to individuals, indicated that the average dose was 2.36 ± 0.88 mSv per year. This level of radiation exposure is relevant when considering safety guidelines and health standards. For context, the average annual effective dose from natural background radiation worldwide is approximately 2.4 mSv. While the values recorded at Erasama Beach are comparable to global averages, the specific context of high radiation areas necessitates careful monitoring to ensure the safety of residents and visitors. Additionally, the study reported an airborne radiation dose rate of 1925 ± 718 $nGyh^{-1}$, a measure that reflects the gamma radiation emitted by naturally occurring radionuclides in the environment. This airborne dose rate is significant because it can affect individuals who may be exposed to radiation while engaging in outdoor activities near the beach or living in close proximity to it. The implications of these findings are multifaceted. First, they underline the necessity of conducting ongoing surveillance and research in high background radiation regions like Erasama Beach. Understanding the radiation levels and their potential health effects can help inform local communities, guiding them in making safe choices regarding their exposure to natural radioactivity. In conclusion,

the analysis of sand samples from Erasama Beach using an HPGe detector highlighted the presence of high activity concentrations of radionuclides, particularly thorium, uranium, and potassium. The study also established that the external effective dose rates and airborne radiation levels were significant, warranting continued monitoring and evaluation of the health impacts on the local population. As awareness of natural radiation levels grows, it becomes increasingly important to ensure that safety measures are in place to protect both residents and visitors in these unique environments (Mohanty et al., 2004).

2.2.2 Radiometric analysis in Kenya

Sindani et al., (2022) conducted a study in Bungoma County, Kenya, wherein samples of sand were gathered from ten chosen rivers. Two samples were collected from each river through a process of random sampling. The investigation utilized a NaI(TI) gamma ray spectrometer with high resolution to determine the activity concentration of ^{238}U, ^{40}K and ^{232}Th. The utilization of the activity concentration of the three primordial radionuclides enabled the computation of diverse radiation exposure parameters, including but not limited to the radium equivalent, yearly effective dose rate, internal and external hazard indices. The research showcased the mean activity concentration of three primordial radioactive nuclides. According to the findings of the study, the measurements of ^{238}U demonstrated a spectrum of values ranging from 0 ± 0.03 Bq/kg to 4 ± 0.24 Bq/kg, with an average amount of 2 ± 0.1 Bq/kg, ^{232}Th ranged from 32 ±1.6 Bq/kg to 87 ± 4.38 Bq/kg with a mean value of 55 ± 2.78 Bq/kg and ^{40}K ranged from 27 ± 1.37 Bq/kg to 76±3.8 Bq/kg, with an average of 51±2.56 Bq/kg. The observed arithmetic means of the activity concentrations for ^{238}U, ^{232}Th and ^{40}K were found to be lower than the global averages of 33 Bq/kg, 33 Bq/kg and 420 Bq/kg respectively. The annual effective dose rate demonstrated a range of

fluctuations in both indoor and outdoor settings, with values ranging from 0±0mSv/y to 0.2±0.01 mSv/y and 0±0.003 mSv/y to 0.1±0.009 mSv/y, respectively. The average annual effective dose rate was found to be 0.1±0 mSv/y and 0.1±0.006 mSv/y for indoor and outdoor environments respectively. The annual effective dose rates were determined to be within the established safe limit of 1 mSv/y. According to this study, the use of sand obtained from specific rivers in Bungoma County, Kenya for construction purposes has minimal health risks for the nearby population and dwellers of buildings constructed from the sand.

According to Wanyama et al., (2020) a research study was conducted to measure the levels of radioactivity in tailings and assess their potential hazards at the Roster man gold mine site in Kakamega. A total of 30 tailing samples were collected, measured, and analyzed using the NaI(TI) detector. The investigation demonstrated that the mean fundamental constituents of ^{40}K, ^{232}Th, and ^{238}U were 262±11.48 $Bqkg^{-1}$, 114±5.78 $Bqkg^{-1}$ and 84±2.64 $Bqkg^{-1}$ respectively, for all the samples. The study established the mean annual effective dose rates for both indoor and outdoor exposure to be 0.4±0.02 $mSvy^{-1}$ and 0.3±0.01 $mSvy^{-1}$, respectively. The average dose rate for both indoor and outdoor exposure was calculated to be 52±65.4 $nGyh^{-1}$. The investigation revealed that the mean radium equivalent activity was 274±12.90 $Bqkg^{-1}$, falling below the established threshold range of 370 $Bqkg^{-1}$, therefore, Roster man's mining poses minimal health risk to the surrounding community.

Kiprono, (2020) conducted a study with the objective of evaluating the activity concentration rates and radiation hazard indicators of soil samples collected from Kericho County. The NaI(Tl) gamma-ray detector was employed for analysing the samples . The measured activity of ^{238}U, ^{232}Th, and ^{40}K exceeded the global average activity, with mean values of 143±7 $Bqkg^{-1}$, 95±4 $Bqkg^{-1}$ and 1086±49 $Bqkg^{-1}$

respectively. The mean radium equivalent, measured at 362±18 $Bqkg^{-1}$, was found to be within the acceptable range as per the reference values. The study yielded mean values of 1.36±0.07 and 0.98±0.05 for H_{in} and H_{ex}, respectively. According to estimates, the typical outdoor absorbed gamma radiation was measured at 169±8 $nGyh^{-1}$and was above the average worldwide value. It was found that the mean annual gamma dose that is effective outside is 0.410.02 $mSvy^{-1}$, which is much less than the amount that the ICRP advises. There is no health danger connected to radiation exposure according to the study results.

The radiometric examination of radionuclides found in rocks and sand from Tyaa river deposits in Kitui County, Kenya, showed that neither the wet nor the dry seasons had levels that were higher than the set threshold limits or values (Matsitsi et al., 2019). The average activity concentrations of ^{40}K, ^{232}Th and ^{226}Ra for rocks and sand respectively, were found to be 659± 33, 46±2.3 and 22±1.1 $Bqkg^{-1}$, 824±41 and 49± 2.5 and 27±1.4 $Bqkg^{-1}$ during the wet season. It was shown that during the dry season, activity concentrations for both rocks and sand were somewhat greater. However, all of the measured values were determined to be within the permitted ranges, suggesting that there is no possible health risk related to radiation exposure for the general population.

In the Mrima Hills Coastal Kenya area, carbonatite rocks were discovered to contain a high amount of background radiation according to a radiological research survey. Researchers used a gamma-ray spectrometer in Mrima-Karuku hills, an area with high levels of background radiation to conduct their research. The activity concentrations of ^{232}Th, ^{40}K, and ^{238}U were ranging between 386±12 and 1817±51 $Bqkg^{-1}$, 235±19 and 603±28 $Bqkg^{-1}$, and 68±6 and 326±24 $Bqkg^{-1}$, respectively. In the air, the absorbed dose rates varied from 60 to 2368 $nGyh^{-1}$, which was much higher than the

permitted limit of 600 $nGyh^{-1}$. This was because the air had significant levels of ^{232}Th activity. The data demonstrated that the region has a high background level of radiation, and as a consequence, the population is exposed to radiation dangers (Kaniu et al., 2018).

Kipngeno, (2015) conducted a study which involved the collection of samples of green tea leaves and soil from Kericho County, Kenya. The samples were subjected to analysis using a NaI(Tl) detector, with the aim of ascertaining the presence of gamma-rays in both the tea leaves and soil. As per the findings, the average activity concentration levels of ^{238}U, ^{232}Th and ^{40}K in Mau tea leaves were 53±3, 40±4 and 558±7 $Bqkg^{-1}$ respectively. Similarly, the Estate's leaves exhibited average activity concentrations of 48±5, 43±2 and 667±8 $Bqkg^{-1}$ for the aforementioned isotopes. The study found that the average activity concentrations of ^{238}U, ^{232}Th and ^{40}K in Mau soil were 51±5, 51±4 and 724±9 $Bqkg^{-1}$ respectively. In contrast, the average activity concentrations of ^{238}U, ^{232}Th and ^{40}K in Estate's soil were 66±8, 55±2 and 819±9 $Bqkg^{-1}$. The annual effective dose rates of soil and tea leaves were found to be 0.12±0.06 and 0.09±0.005 $mSvy^{-1}$ respectively. These values were observed to be below the permissible limit, thereby signifying that the utilization of tea leaves and soil is safe.

Elsewhere in Kitui, a radiological survey was conducted to analyze the suitability of Kitui south limestone (Mulwa et al., 2013). The study employed a hyper-pure germanium detector with an external diameter of 76 mm and an active volume of 144 cm^3 to measure and evaluate 45 samples. The results indicated that the activity concentrations of ^{226}Ra, ^{232}Th, and ^{40}K were below the global averages of 50 $Bqkg^{-1}$, 50 $Bqkg^{-1}$ and 500 $Bqkg^{-1}$ respectively. The investigation revealed that the levels of radiation hazards, specifically the External Hazard Index (EHI), Gamma Activity

Index (GaAi), and Alpha Index, were found to be below the established threshold limits by a margin of less than one unit Therefore, considering that the radioactive equivalent is below the acceptable threshold, it can be concluded that limestone can be employed as a building material without posing any health hazards to individuals.

A research investigation was carried out in the Migori Artisanal Gold Mine Belt situated in the Nyanza South region, utilizing NaI(TI) gamma-ray spectrometry as a means to determine the concentration of radioisotopes, specifically ^{226}Ra, ^{232}Th and ^{40}K (Odumo et al., 2011). The specimens displayed diverse levels of radioisotope activity concentrations of ^{226}Ra, ^{232}Th, and ^{40}K radioisotopes, with values ranging from 21 to 258 Bqkg^{-1}, 12 to 145 Bqkg^{-1} and 80 to 413 Bqkg^{-1} respectively. The absorbed dose rate in air of ionizing radiation exhibits a range of 16 to 178 nGyh^{-1}, averaging at a value of 42 nGyh^{-1}. The results suggest that radioisotopes contribute to radiation exposure among the general population.

A radiological study of the Tabaka soapstone quarry in Kisii region which involved the collection of 14 soil and rock samples were analyzed with a high-resolution gamma detector by Kinyua et al., (2011). There were 541.4 and 43 nGyh^{-1} absorbed dose rates above and below the ground respectively. In terms of ^{232}Th, ^{226}Ra and ^{40}K, the average activity concentrations were 155.15, 201.55 and 1012 Bqkg^{-1}. The mean yearly effective dose rate was 0.44 mSvy^{-1} which corresponded to an increased cancer incidence risk of 0.07%. The internal and external risk factors, both surpassed the 1unit limit. There was a 0.56 mSvy^{-1} difference between the yearly effective dose rate and 1 mSvy^{-1} and because of the soapstone's very high average absorbed dose rate in the air (177.6 nGyh^{-1}), it could not be used safely.

A radiological survey was conducted by Achola, (2009) in the Lambwe East region of Western Kenya, forming part of a doctoral dissertation at the University of Nairobi. This study aimed to evaluate the levels of natural radiation in the area, particularly focusing on the geological formations present. To carry out the measurements and analyses, the research utilized a high-purity germanium (HPGe) gamma-ray detector, a sophisticated instrument known for its accuracy in detecting and quantifying various radionuclides. A total of 21 rock samples were collected from the Lambwe East region for analysis. The use of the HPGe detector allowed for precise measurements of gamma radiation emitted from these samples, providing a comprehensive understanding of the radiological characteristics of the area. The findings from the survey revealed that the average annual external effective dose rate was calculated to be 5704.78 μSv y^{-1}. This value indicates a significant level of radiation exposure for individuals in the region, highlighting the potential health risks associated with prolonged exposure to such high levels of natural radiation. The geographical area studied was classified as a High Natural Background Radiation Area (HBRA). This classification is essential as it underscores the unique radiological environment of Lambwe East, which is influenced primarily by the presence of carbonite rock formations. These rock formations are known to contain naturally occurring radioactive materials that contribute to the overall radiation levels in the region. The predominance of carbonite rocks in the area serves as a key factor in the elevated radiation exposure observed. The implications of Achola's study are significant for both public health and environmental monitoring. Understanding the radiation levels in HBRA is crucial for assessing potential health risks to local communities and for establishing safety guidelines for exposure. The findings can inform local authorities and health officials about necessary precautions and interventions to minimize

radiation exposure among residents. In summary, Achola's radiological survey in the Lambwe East region of Western Kenya utilized advanced gamma-ray detection techniques to analyze 21 rock samples. The results indicated a high annual external effective dose rate of 5704.78 μSv y^{-1}, classifying the area as an HBRA primarily due to the influence of carbonite rock formations. These findings emphasize the importance of ongoing monitoring and research in regions with elevated natural radiation levels to ensure the safety and well-being of the local population

2.3 Theoretical Framework

Gamma ray interaction with matter and biomatter, gamma ray spectroscopy and spectrometry system, energy calibration and resolution, radiation field quantities and secular equilibrium are discussed below.

2.3.1 Gamma Ray Interaction with Matter

When gamma rays come into contact with matter, there are three primary interaction methods that can take place ; photoelectric absorption, Compton scattering, and pair production as shown in Figure 2.1.

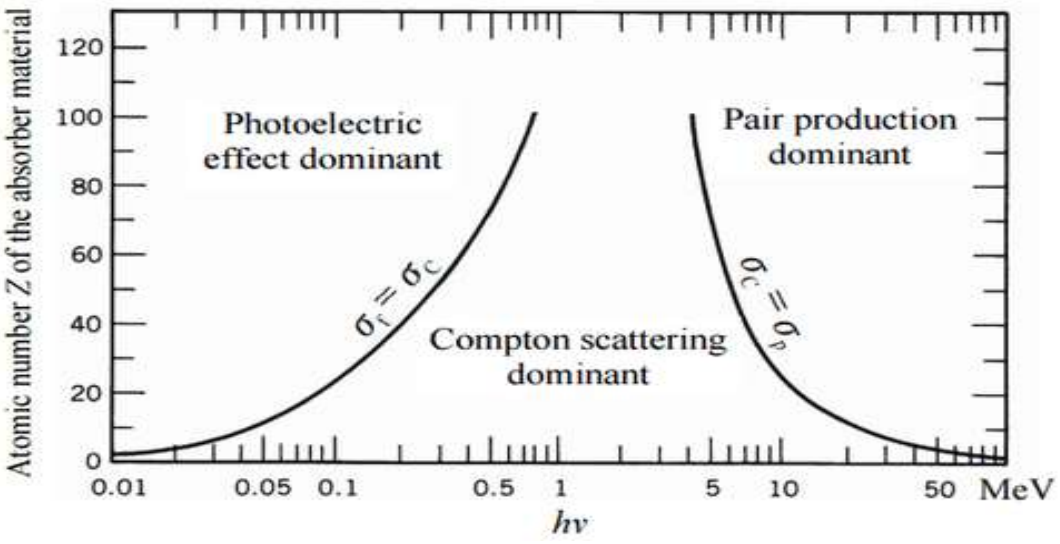

Figure 2.1: Photon interaction process with matter (IAEA, 2005).

Figure 2.1 illustrates that photoelectric interaction takes over control in a region with lower photon energy and higher atomic number. The Compton scattering dominates in the region of low atomic number and moderate photon energy. Pair production dominates in high photon energy and high atomic number region.The energy provided is sufficient for conversion of a gamma ray to an electron and a positron (IAEA, 2005).

2.3.1.1 Photoelectric absorption

In this case, a gamma-ray interacts with an atomic electron that is tightly bond to the nucleus, usually the K-shell electron, and all energy is lost as shown in Figure 2.2

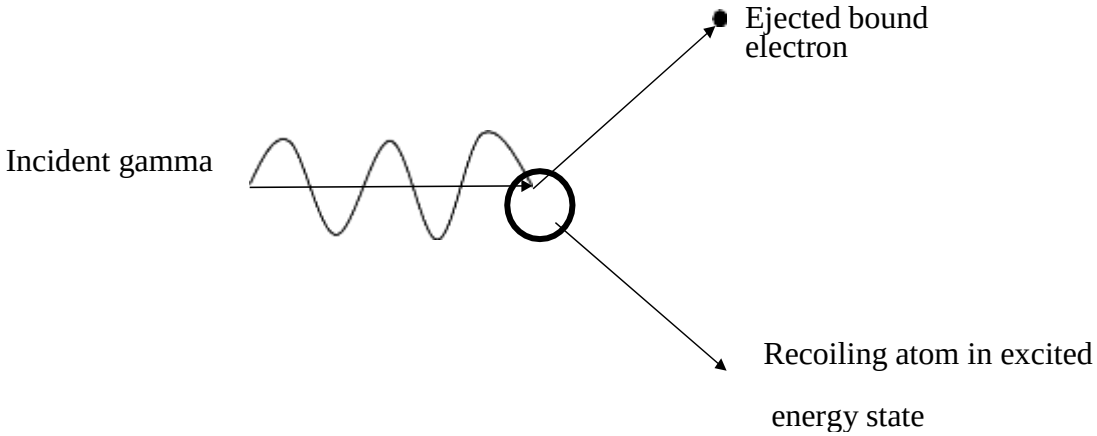

Figure 2.2: A diagrammatic illustration of the phenomenon of photoelectric absorption (Ragheb, 2011)

Photon energy is used to ionize the atom and the remainder is to accelerate the photoelectron. During the removal of photoelectron, incident photon is completely absorbed hence contributing to the attenuation of the X-ray beam as it passes through matter. Photoelectric absorption is the major contributor to the beam attenuation upto ≈ 30keV when human tissues (Z = 7.4) are irradiated. The photoelectric process is dependent on photon energy and atomic number as shown in equation (2.1)

$$\tau \propto \frac{Z^3}{E^3} \qquad (2.1)$$

Where τ denotes the probability of occurrence of photoelectric (PE) interaction, Z denotes the atomic number and E is the energy of photon.

Gamma photon energy is divided into 3 components when it interact with an atom and is expressed by the relation shown by equation 2.2 (Ragheb, 2011).

$$E_\gamma = E_e + E_a + E_b \quad (2.2)$$

Where E_γ signifies the initial gamma photon's kinetic energy, E_e denotes the free electron's kinetic energy, E_a denotes the recoiling atom's kinetic energy, and E_b denotes the electron's binding energy within the atom.

2.3.1.2 Compton scattering

In this process, gamma-ray interact with free bound electron or weakly bound electron or outermost or valence electron ($E_\gamma >> E_b$) and elastically scatters from it as shown in Figure 2.3

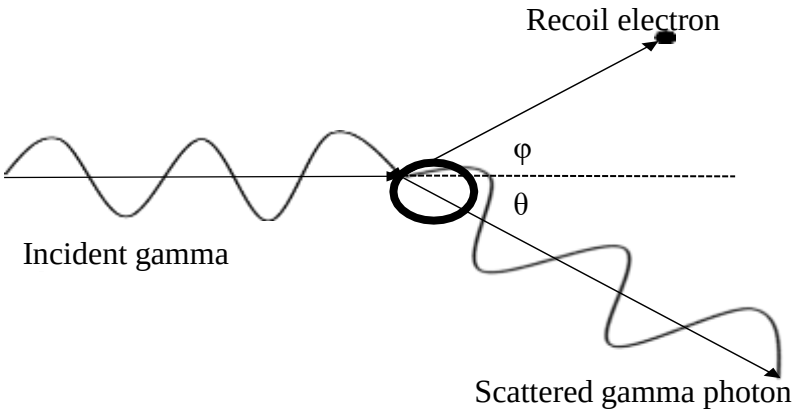

Figure 2.3: A schematic representation of the Compton scattering process (Ragheb, 2011).

The energy of the scattered gamma photon decreases when the angle (θ) of scattered photon increases thus when incident photon energy is higher, there will be a greater percentage energy loss. Compton effect dominates when human tissues are irradiated between the energy range of 30 keV and 30 MeV which is diagnostic and

therapeautic radiation range. The relation between Compton effect and the number of outer shell electrons is direct but weakly depends on photon incident energy and doesn't depend on the atomic number. Equation (2.3) provides the expression for the energy of the electron that has undergone scattering (Ragheb, 2011).

$$E_e = E_\gamma - E' \tag{2.3}$$

Where the energy of the scattered gamma rays is denoted by E′.

The energy of the scattered gamma-ray is expressed by the equation 2.4 as follows (Ragheb, 2011).

$$E' = \frac{m_0 c^2}{1 - \cos\theta + \frac{m_0 c^2}{E}} \tag{2.4}$$

Where m_0c^2 is the rest energy of the electron, equals 511 keV and θ is the angle formed between the incident and scattered gamma-ray (See Figure 2.3).

2.3.1.3 Pair production

The pair production interaction process occurs when a photon undergoes interaction with a nucleus, resulting in the disappearance of the photon and the formation of an electron-positron pair as a consequence of the interaction. During the liberation of electron and positron, electron is absorbed while as positron comes to rest, it combines with the neighboring electron and neutralize a process known as annihilation. The minimum threshold energy for pair creation by a photon is 1.02 meV, which is equivalent to the combined mass of two electrons, or $2m_0c^2$. When the energy exceeds 1.02 meV, the surplus energy is distributed between the electron and positron in the form of kinetic energy (Ragheb, 2011). For energy to be conserved, equation (2.5) holds (Ragheb, 2011).

$$E_\gamma = h\nu = E_e = E_p = 2m_0c^2 \quad (2.5)$$

Equation (2.6) shows the condition for occurrence of pair production (Ragheb, 2011).

$$E_e + E_p = 0 \quad (2.6)$$

Therefore the minimum energy for pair production becomes,

$$E_{\gamma min} = h\nu_{min} = 2m_0c^2 = 2 \times 0.51 = 1.02 \text{ meV} \quad (2.7)$$

The probability of pair creation is directly proportional to the increase in photon energy and atomic number Z. This relationship is expressed in equation (2.8), where it is noted that the likelihood of pair creation increases proportionately with the square of atomic number Z (Ragheb, 2011). Figure 2.4 shows the schematic diagram of the formation of a pair of electron – positron.

$$\sigma_{pp} \approx Z^2 \quad (2.8)$$

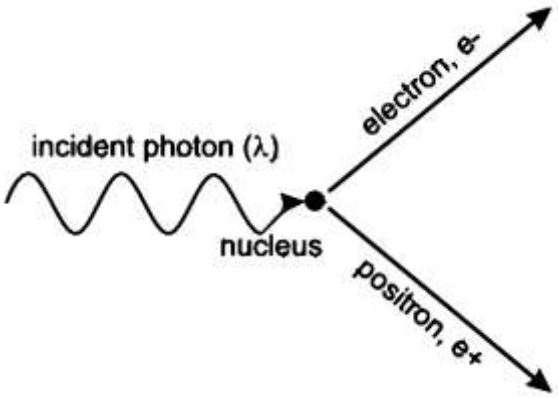

Figure 2.4: A schematic diagram showing the formation of an electron-positron pair (Ragheb, 2011).

During positron decay, nuclear transmutation occurs, which can lead to negative risk effects, despite the relatively low level of radiation associated with this type of decay process

2.3.2 Gamma-ray interaction with Bio matter

The effects of ionization of radiations on biomatter are dependent on the intensity of energy deposited on tissues of living organism and are assessed by absorbed dose, D, and equivalent dose H. The absorbed dose refers to the amount of energy that is absorbed by a material per unit mass. It is a quantification of the energy that is transferred to matter as a result of its interaction with an ionizing radiation field.

The equivalent dose can be defined as the multiplication of the dose and a modifying factor, commonly known as the quality factor (QF). The QF is utilized to reflect the radiation's relative biological effectiveness.

$$H_T = D \times QF \tag{2.9}$$

Effective Dose Equivalent (EDE) is the weighted average of the individual doses to many vital tissues.

$$H_E = \sum_T H_T \times W_T \tag{2.10}$$

(Sum is overall tissues) (ICRP, 2005)

2.3.3 Gamma Ray Spectroscopy

Naturally occurring radionuclides emit gamma rays at distinctive energies that when counted form representative photo peaks. A gamma ray spectrometry system is used for detecting and counting gamma ray events which can help in determining the quantities of given radionuclide in materials. In this section, a Sodium Iodide Thallium doped (NaI(Tl)) gamma ray spectrometry system which was used for gamma counting is described. The NaI(Tl) detector works based on scintillation mechanism (ICRP, 2005).

2.3.4 NaI(TI) Gamma Ray Spectrometry System

The spectrometry system mainly comprises of detection, signal processing unit and a multichannel analyser (MCA) which has 1024 channels. Gamma rays are detected by means of scintillation process where the atoms of NaI(TI) crystal are excited to higher energy states upon interaction with gamma rays (ICRP, 2005). When an object loses energy and transitions to lower energy states, it emits visible light. This light causes the dislodgement of electrons from the photocathode through the photoelectric effect. Electrons undergo acceleration within the photomultiplier tube (PMT) by means of a high potential ranging from several hundred volts to 1.2 kilovolts, which is applied between the cathode dynodes and anode. As more electrons are ejected from each successive dynode in the PMT, an electric current is produced and fed into an amplifier before being processed to determine incident photon's energy associated with the electric pulse (ICRP, 2005). Figures 2.5 and 2.6 below show the different parts of the gamma ray measurement system and a pictorial presentation of the detector respectively.

Figure 2.5: Parts of NaI(TI) Gamma Spectrometer (ICRP, 2005)

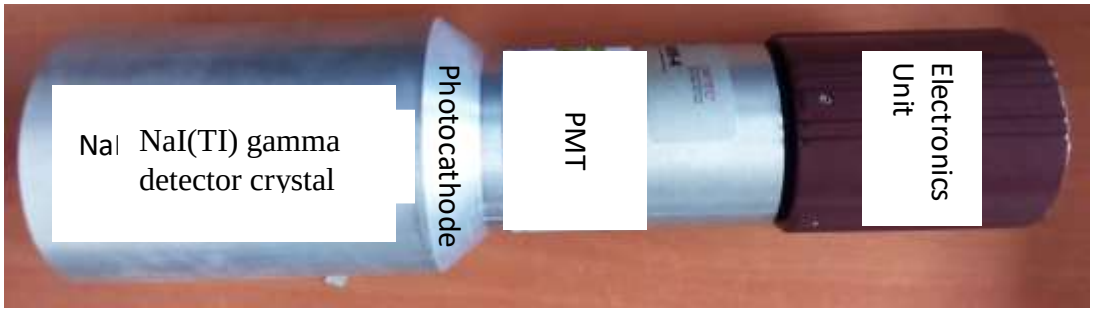

Figure 2.6: A schematic diagram of NaI(TI) detector (ICRP, 2005)

All the counted energies are displayed discriminatively on a computer screen through a MCA software. In the current study, an ORTEC based Maestro software and a USB Digi-base signal processing unit and amplifier were used. Importantly, the unit also houses the high voltage converter which increases the 5 V USB input from PC to the 800 V that was used as the optimal PMT voltage (ICRP, 2005).

2.3.5 Energy Calibration .

Energy calibration is a crucial component in gamma spectrometry studies, as it establishes a relationship between the channels of the detector and the corresponding gamma-ray energies (Matsitsi et al., 2019). To achieve accurate calibration, known photo peaks from specific artificial gamma-ray emitters were utilized. These include Americium-241 (Am-241) at 60 keV, Cesium-137 (Cs-137) at 662 keV, and Cobalt-60 (Co-60) at two energy levels, specifically 1173 keV and 1332 keV. By using these known energy values, an energy-channel fitting function was developed, enabling the direct identification of the energy of a particular peak based on its channel number (ICRP, 2005). This calibration process is essential for ensuring precise measurements and interpretations of the gamma radiation detected. Figure 2.7 below illustrates the energy calibration curve, which demonstrates a perfect coefficient of correlation, $R^2 = 1$. This indicates an ideal linear relationship between the channel numbers and their respective gamma-ray energies, confirming the reliability of the calibration method employed in the study. Such accuracy is vital for assessing radiation levels and potential health risks associated with radioactive materials

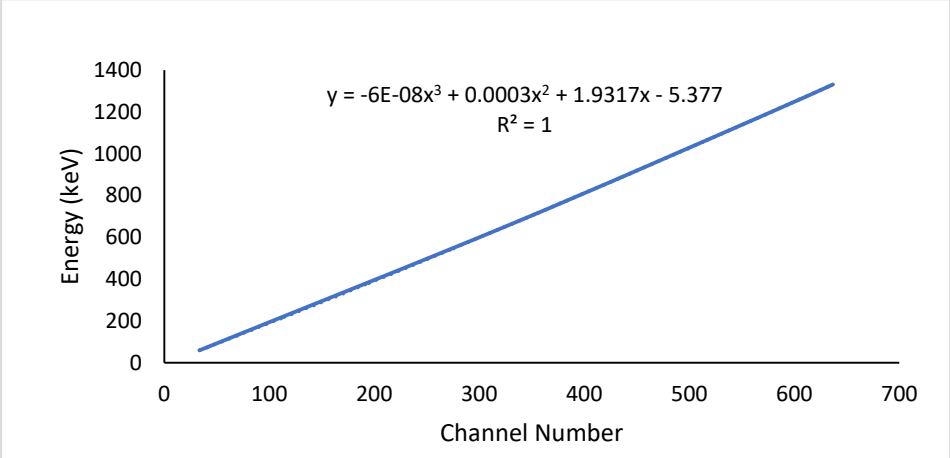

Figure 2.7: Schematic diagram of Energy Calibration in a NaI(TI) Detector

2.3.6 Energy Resolution

The proximity of photo peaks in a sample is influenced by the specific radionuclides present, making it essential to use a detector with considerable resolution to differentiate between them effectively. The ability of a detector to distinguish these photo peaks is referred to as its energy resolution. As illustrated in Figure 2.8 below, the energy resolution of the NaI(TI) detector exhibits high performance at lower energy levels but gradually decreases as the energy increases. This characteristic means that the peaks associated with higher energy are broader, making them less distinct, while the peaks corresponding to lower energy are narrower and more sharply defined. To determine energy resolution, one calculates the ratio of the full width of the peak at half maximum (FWHM) to the centroid energy. This ratio serves as a critical measure in evaluating the detector's effectiveness in accurately identifying and quantifying the different radionuclides present in a given sample.

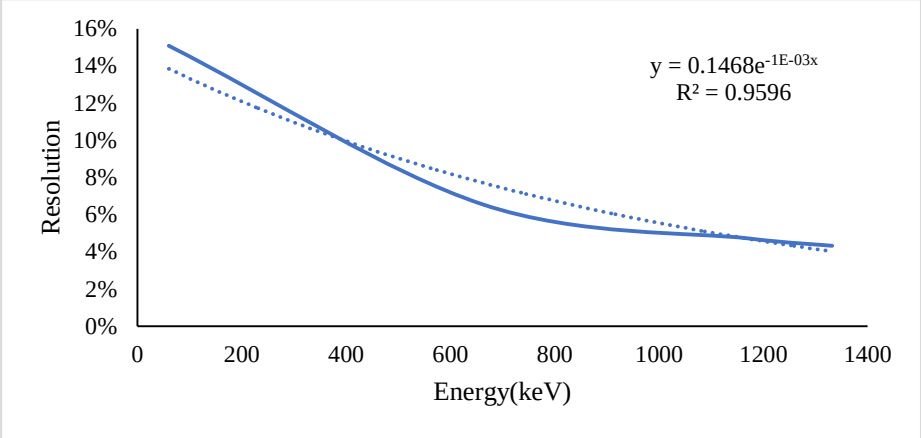

Figure 2.8: Schematic Diagram of the Gamma Ray Spectrometer Energy Resolution

(ICRP, 2005)

The energy resolution of the NaI(TI) detector can therefore be expressed by equation 2.11.

$$\text{Energy Resolution} = \frac{\text{FWHM}}{\text{Photon Energy}} \tag{2.11}$$

where FWHM is Full Width at Half Maximum

2.4 Radiation field quantities

The radiation field quantiries are parameters utilized to characterize the properties of a radiation beam and its corresponding dose. These field quantities are radiant energy, particle fluence,energy fluence and kinetic energy liberated per unit mass. Radiation field quantities are essential parameters used to characterize the properties of a radiation beam and to assess its corresponding dose. Understanding these quantities is crucial for various applications, including medical treatments, radiation protection, and nuclear safety.

2.4.1 Radiant energy (R)

Radiant energy is the energy of particles that are either radiated, transmitted or received. It refers to the total energy carried by the radiation beam. This energy is pivotal in determining the potential impact of radiation on matter, including biological tissues and is given by equation (2.12). (Seuntjens et al., 2005).

$$R = E \times N \tag{2.12}$$

where R is radiant energy, E is the particles' energy and N is the number of particles.

2.4.2 Particle fluence (ϕ)

It is the ratio of the number of incident particles on a matter to the area. Its unit is m^{-2}

It is defined as the number of particles passing through a unit area. This measure helps quantify the intensity of the radiation field and is significant in evaluating exposure levels.

$$\phi = \frac{dN}{dA} \tag{2.13}$$

where dN is the number of incident particles on a matter of area dA (Seuntjens et al., 2005)

2.4.3 Energy fluence (Ψ)

It is the ratio between radiant energy and the area. Its unit is $Jm^{-2.}$ It represents the total energy deposited by the radiation in a unit area. This parameter is vital for understanding how much energy is absorbed by materials or tissues, influencing both the effectiveness and safety of radiation applications.

$$\Psi = \frac{dR}{dA} \tag{2.14}$$

where dR is the radiant energy incident on a matter of area dA.

The relationship between energy fluence and particle fluence is shown in equation (2.15)

$$\Psi = \frac{dN}{dA}E = \phi E \tag{2.15}$$

where dN represents the number of particles with energy E (Seuntjens et al., 2005).

2.4.4 Kinetic energy released per unit mass (Kerma)

It is the kinetic energy of ionizing radiation absorbed by matter per unit mass and is measured in grey (Gy). This quantity is crucial for assessing the biological effects of radiation, as it directly relates to the energy available to cause ionization and other damage within cells.

$$K = \frac{dE_{tr}}{dm} \tag{2.16}$$

where $dE_{tr\ is}$ the mean kinetic energy of ionizing radiation and dm is the mass of a given material (Seuntjens et al., 2005).

2.5 Secular equilibrium

One notable instance of this phenomenon occurs when the half-life of the parent radioisotope is considerably longer than that of the daughter radioisotope. In such cases, both isotopes can decay simultaneously, but the behavior of the daughter isotope is heavily influenced by the decay of the parent isotope. When the system reaches a state known as secular equilibrium, the quantity of the daughter radioisotope, denoted as D, becomes directly dependent on the amount of the parent radioisotope, represented as P, as well as their respective half-lives.In this equilibrium

state, the rate at which the daughter radioisotope accumulates is balanced by its decay rate, leading to a relatively stable concentration over time. The relationship between the two isotopes can be quantitatively expressed through an equation that describes the rate of change of the number of daughter radioisotopes, denoted as D. This mathematical representation, found in equation (2.17), illustrates how the dynamics of radioactive decay govern the behavior of both the parent and daughter isotopes over time. Understanding these relationships is essential for applications in radiometric dating, nuclear medicine, and various fields of nuclear science (Pavan & Andrew, 2020).

$$\frac{dN_D}{dt} = \lambda_P N_P - \lambda_D N_D \tag{2.17}$$

At a given moment, N_P and N_D denote the quantities of atoms present in the parent and daughter radioisotopes respectively, whereas λ_P and λ_D correspond to the decay constants.

2.6 Identification of knowledge gap

In Kenya, cancer cases and mortality rates have been alarmingly high, making cancer the third leading cause of death, following infectious diseases and cardiovascular conditions. Prolonged exposure to radiation emitted from naturally occurring elements such as radon, uranium, thorium, and potassium is recognized as the second leading cause of lung cancer. These radioactive isotopes are commonly found in the Earth's crust, as well as in soil, rocks, food, and water sources. The pervasive presence of these materials underscores the importance of monitoring and managing radiation exposure, as they can significantly impact public health and contribute to the rising cancer rates observed in the country. A series of studies have indicated that various geological characteristics significantly influence radiation levels in different regions

of Kenya. Certain areas are classified as high background radiation zones, primarily due to the presence of carbonatite and monazite rocks, which emit elevated levels of radiation. These geological formations are known to contain naturally occurring radioactive materials that contribute to the overall radiation exposure in their vicinity. Understanding the relationship between geology and radiation levels is essential for assessing potential health risks and for implementing appropriate safety measures to protect residents living in these high radiation areas, thereby ensuring public health and safety. From the existing data and literature on the number of radiations in construction materials in Kenya, Mrima hills (Coastal region), Mrima-Karuku hills (Coastal region), Lambwe East Location (South Western region), and Migori Artisanal Gold Mine (Nyanza region) were reported to be having elevated levels of radiations, therefore considered as high background radiation areas. The populace in these areas is facing radiations health risks. Tyaa River (Kitui), Kitui South Limestone (Kitui), and Rosterman Gold Mine Site (Kakamega) were reported to be regions of normal radiation background areas and are posing no health risk of radiations to the populace. There being limited data and literature review on the levels of radiations from the primordial radioisotopes and their decay products in the rocks used for construction excavated in Kericho County the research gives information on the radiation levels. The study utilized gamma-ray spectrometry as a primary method for analyzing the radioactivity levels in the rocks excavated from Kericho County. The results obtained from this analysis will play a crucial role in assessing the safety of these rocks for construction and other uses. By determining the levels of natural radioactivity, the study will also facilitate the classification of Kericho County as either a high background radiation area or a normal background radiation area. This classification is essential for evaluating potential health risks associated with exposure

to radiation for the local residents and the surrounding communities. By providing clear and scientifically-backed insights, the study aims to inform public health policies and safety regulations, thereby ensuring the well-being of the inhabitants of Kericho County and beyond. Ultimately, the findings will contribute to a better understanding of environmental safety and the management of natural resources in the region.

CHAPTER THREE

MATERIALS AND METHODS

3.1 Introduction

This chapter provides details regarding the study area, materials, and apparatus employed for collecting samples, preparing the samples, gamma-ray spectrometry, sample analysis and the methodology employed for determining radiation hazard indices.

3.2 Study Area

The study was conducted in quarries located in Kericho County, situated in the southern rift region of the Great Rift Valley, at a distance of approximately 256 kilometers from Nairobi, the capital city of Kenya. The cartographic depiction of Kenya is shown in Figure 3.1.

Kericho County encompasses a geographical area of 2,111 square kilometers, positioned at longitudinal coordinates of 35°02′ and 35°40′ east, along with an equatorial latitudinal coordinate of 0°23′ south. The county's elevation is approximately 2,002 meters above sea level, providing it with a unique topography. According to the estimates from the 2019 Kenya Population and Housing Census, the population of Kericho County is approximately 901,777 individuals. This diverse population contributes to the region's vibrant communities and plays a significant role in the county's socio-economic development. The combination of its geographical features and population density influences various aspects of life in Kericho County, including agriculture and industry.

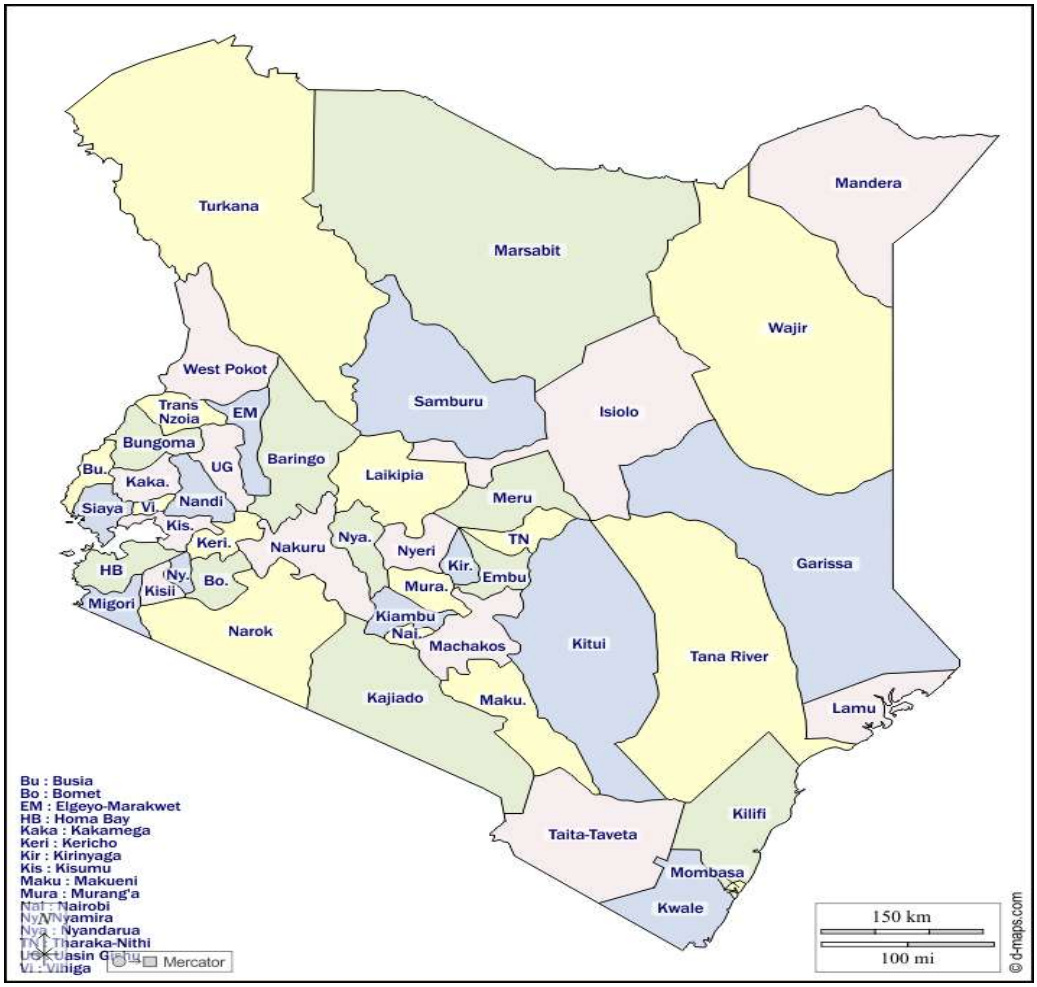

Figure 3.1: Map of Kenya (IEBC, 2013).

The study involved the collection of samples from several quarries situated in diverse regions of Kericho County, Kenya. The quarries selected and their respective sub-counties are as follows; Kedowa(Q1), United(Q2), Kipsirichet(Q3) and Jagoror(Q4) in Kipkelion East, Kimondui(Q5) and Tunnel(Q6) in Kipkelion West, Kisumu Concrete(Q7), Rai cement(Q8) and Rockland(Q9) in Soin-Sigowet, Laliat(Q10) and Chepsetion(Q11) in Ainamoi, Kibingei(Q12) in Belgut, Kibugat(Q13), Maburo Kipwastuiyo(Q14) and Agisiek(Q15) in Bureti sub-county. These areas were chosen due to the fact that a significant proportion of the populace residing in Kericho County, as well as the neighbouring counties, depend on the rocks present in those localities for the purpose of constructing buildings. Consequently, it is imperative to

carry out research aimed at determining the levels of primordial radionuclides that are present in construction rocks, in order to guarantee the safety of building materials utilised in the construction of both residential and commercial edifices that are occupied by individuals.

The cartographic depiction of the area under investigation is shown in Figure 3.2.

Figure 3.2: Map of Kericho County (IEBC, 2013)

3.3 Research Materials and Instruments

The study employed a variety of materials and equipment to effectively collect, measure, and analyze the rock samples. Essential apparatus included gloves to ensure safety during handling, along with mobile phones equipped with GPS technology for accurate location tracking of sample collection sites. A total of thirty 1000 ml plastic containers and thirty 300 ml plastic containers, each labeled with stickers for easy

identification, were used to store the samples. Additionally, metallic buckets facilitated the transportation of larger quantities of materials. For sample preparation, a rock crusher and a 1 mm mesh sieve were utilized to achieve the desired particle size. An electronic weighing balance ensured precise measurements of sample masses. A hot air oven was used for drying, while aluminum foil helped in sample preservation. The study also incorporated IAEA reference materials for calibration purposes, along with packing tape for secure packaging. Finally, a Gamma-ray spectrometer, specifically a Thallium-activated Sodium Iodide detector, was employed to measure the radioactivity levels, and a gas mask was included for protection during potentially hazardous tasks.

3.4 Sample distribution and collection

3.4.1 Sample distribution

Systematic random sampling was used while collecting samples from the designated quarries as per the requirements of IAEA. The county's quarry locations were determined by geological distribution and the availability of building rocks. Random methodology was used to collect two samples at a depth of 100 cm from each quarry, increasing sensitivity and providing representative composite samples for better representation, following IAEA sampling regulations and recommendations (IAEA, 2004). There were a total of 30 samples taken.

3.4.2 Sample Collection

Two rock samples, each weighing 200 grams, were obtained from the same quarry to ensure consistency in the analysis. These samples were carefully placed in a plastic container with a volume capacity of 1000 milliliters, and were subsequently packaged and identified with distinct codes, that is, R_1Q_1 Meaning Rock Sample1 Quarry1,

R_2Q_1 Meaning Rock Sample2 Quarry1, R_1Q_2 Meaning Rock Sample1 Quarry2, R_2Q_2 Meaning Rock sample2 Quarry2, R_1Q_3 meaning Rock Sample1 Quarry3, R_2Q_3 meaning Rock Sample2 Quarry3 and the rest follow the sequence.

3.5 Sample preparation

The collected samples were subjected to an initial process of crushing, after which a sieving procedure was carried out using a wire mesh. Following this, the specimens underwent a desiccation procedure within a thermal chamber adjusted to a temperature of 105 °C over a period of 24 hours. Following this, the specimens were measured and put in plastic containers with a capacity of 300 ml. In order to prevent the escape of uranium, radon, and thorium, the canisters were properly covered in aluminum foil and secured with rubber bands. As per the recommendation of Mohanty et al., (2004) the specimens were subjected to a four-week storage period to attain a state of secular equilibrium between Ra-226 and Th-232.

3.6 Gamma-ray spectroscopy

The radionuclides ^{238}U (^{226}Ra), ^{232}Th and ^{40}K were evaluated by means of the γ-peak of ^{214}Pb (352 keV), ^{212}Pb (239 keV) and the standard 1460 keV γ-peak respectively, utilizing a NaI(TI) gamma-ray spectrometer. Before sample measurements, environmental gamma background spectra count was determined using a distilled water inside a plastic bottle with similar measurement conditions and later subtracted from a sample measurement. The in-built specialized software was utilized in analyzing the measured gamma-ray spectrum, fitting all major photopeaks simultaneously and generating a menu-driven report that includes the centroid, intensity, and breadth of recognized and undetermined peaks. The gamma-ray energy is proportional to the element and its isotopes, while the counts are proportional to the radioactive source or material's abundance.

Two samples were analyzed each day, with each sample being monitored for a duration of 8 hours using a detector to ensure accurate measurements of radioactivity levels. The spectrum obtained was as shown in Figure 3.1 below.

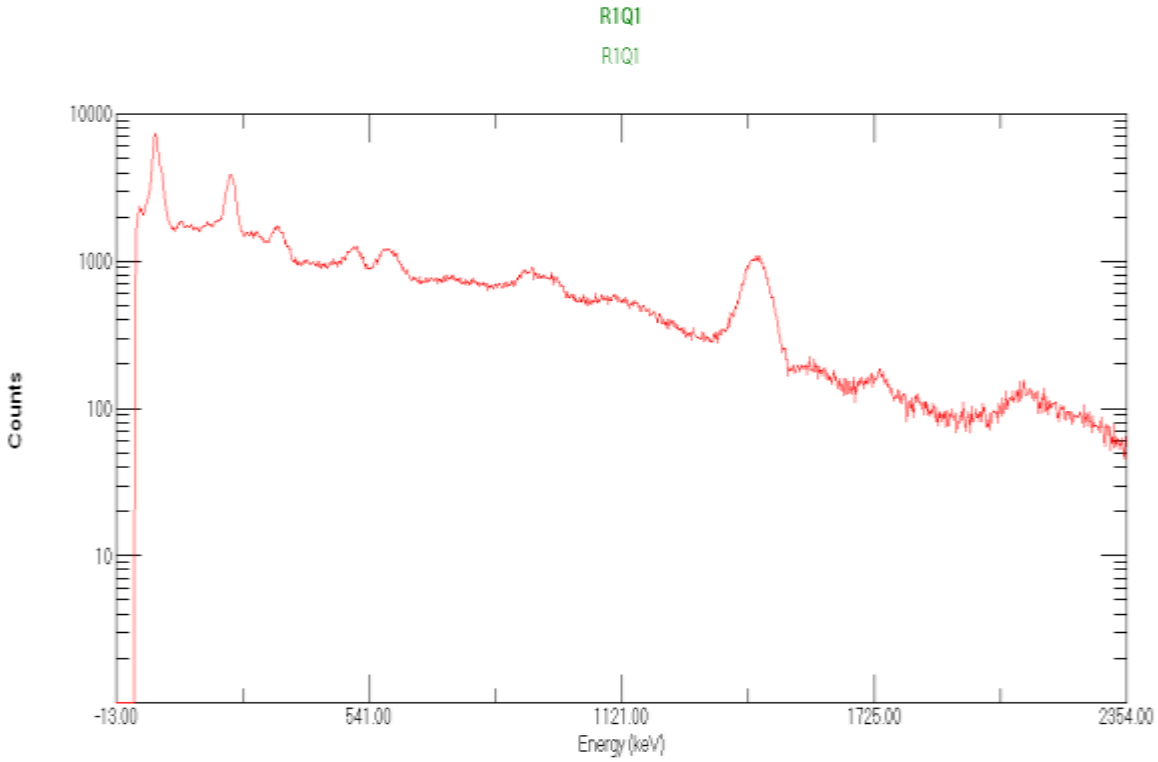

Figure 3.3: Spectrum obtained for sample R_1Q_1

3.7 Background Correction and Uncertainty

From literature, there is a background radiation count emanating from different sources of radiation. Background radiation inside the measurement chamber contributes to radiation count. The ORTEC MCA spectrum analyser software automatically subtracts background radiation count with the help of a built-in determination algorithm. Upon selecting a region of interest (ROI) in the spectrum, it is considered that the counts of first three lower and last three upper background channels of the ROI are critical in the background correction algorithm i.e., if the ROI

channel limits are L and U and that C_x is the counts of channel x within the range of L and U, the net count is deduced by equation 3.1 below (Mulwa et al., 2013)

$$\text{Net count} = \text{Gross count} - \text{Background count} \tag{3.1}$$

Where;

$$\text{Gross count} = \sum_{X=L}^{U} C_X \tag{3.2}$$

$$\text{Background count} = \frac{\sum_{X=L-3}^{L-1} C_X}{3} + \frac{\sum_{X=U+1}^{U+3} C_X}{3} \times \frac{U - L}{2} \tag{3.3}$$

To correct the gross count from the geological specimen, the background count was determined. Since the deionized water was ran similar to the geologically collected samples from the quarries, some counts were noted as shown in Table 3.1.

Table 3.1: Deionized water spectrum information

Nuclide	centroid Energy KeV	Live Time(S)	Real Time (S)	Mass (kg)	Net Area
Th-232	246.0	28796.8	28800	0.25	82±301
U-238	357.8	28796.8	28800	0.25	56±184
K-40	1469.9	28796.8	28800	0.25	11352±478

From Table 3.1, the net areas and the associated centroid energies observed were subtracted from all the geological spectra samples produced by the multichannel analyzer. This subtraction process was essential to derive the net count, which represents the actual counts of the radionuclides present in the samples, free from background radiations.

3.8 Sample analysis

3.8.1 Natural activity concentrations

To accurately measure the activity concentration of the rock samples, they underwent gamma counting using a lead-shielded NaI(TI) gamma detector for a duration of approximately 8 hours. This extended counting period was specifically chosen to ensure the clarity of the observed photo-peaks in the gamma spectrum. To determine the activity levels of the Naturally Occurring Radioactive Materials (NORMs) within the samples, the comparison technique outlined in equation (3.4) by Sangura & Waswa, (2012) was employed. This method facilitates the quantification of radioactive isotopes present in the rock samples by comparing their gamma emissions to known standards.

$$\frac{\mathbf{M_r AC_r}}{\mathbf{I_r}} = \frac{\mathbf{M_s AC_s}}{\mathbf{I_s}} \qquad (\mathbf{3.4})$$

In equation (3.4), the variables M_r, AC_r, I_r, M_s, AC_s, and I_s correspond to reference's mass, reference's activity concentration, reference's intensity, sample's mass, sample's activity concentration and sample's intensity respectively. The equation necessitates that samples be placed in a container with the same shape as that of the reference material. After correcting for background radiation in the obtained spectra, the activities of K-40, U-238, and Th-232 were determined using gamma peaks centered at 1460 keV, 352 keV and 239 keV for each respectively. The activities of IAEA certified reference materials used for activity determination are presented in Table 3.2.

Table 3.2 *:* Parameters of Reference Materials (IAEA, 2005)

IAEA Certified Reference Materials		
Reference	**Energy (KeV)**	**Reference Activity (Bq/kg)**
RGK-1	1460	14000
RGTh-1	239	3250
RGU-1	352	4940

3.8.2. Radiation hazard indices

There are two radiation hazard indices namely external and internal hazard index.

i) External hazard index (H_{ex})

To assess the external exposure to gamma radiation generated by naturally occurring radionuclides present in construction rocks, external hazard index was calculated. This index serves as a critical measure for evaluating potential radiation risks associated with the materials used in construction. If the value of the external hazard index is found to be less than one, it is interpreted to mean that the consequences of exposure to gamma radiation are negligible. This indicates that the levels of radiation in the construction rocks pose minimal risk to individuals who may come into contact with them during construction activities or subsequent use of buildings.

The index is calculated using equation (3.5), (Tsai et al., 2008):

$$H_{ex} = \frac{AC_{Ra}}{370} + \frac{AC_{Th}}{259} + \frac{AC_{K}}{4810} \tag{3.5}$$

ii) Internal hazard index (H_{in})

The inhalation of radionuclides originating from terrestrial sources, specifically ^{40}K, ^{232}Th and ^{238}U (^{226}Ra) present in construction rocks, has been found to result in

internal harm. (Tsai et al., 2008). It was calculated using equation (3.6) (Amrani & Tahtat, 2001):

$$H_{in} = \frac{AC_{Ra}}{185} + \frac{AC_{Th}}{259} + \frac{AC_{K}}{4810} \quad (3.6)$$

According to ICRP, (2005), when the value is lower than one, the radiation's effects on human organs are considered to be insignificant.

3.8.3 Activity utilization index (I_{yr})

The activity utilization index plays a crucial role in assessing the safety of individuals who may be exposed to radiation from construction rocks. This includes miners working at the extraction sites, as well as masons and construction workers involved in building both commercial and residential structures using these materials. By calculating the activity utilization index, researchers can evaluate the potential radiological hazards associated with these rocks, thereby ensuring that safety measures are in place to protect those who work with or around them. A lower activity utilization index suggests a reduced risk of harmful exposure, thereby promoting safer working conditions in the construction industry. It was calculated using equation (3.7) (Risica & Nuccetelli, 2001):

$$I_{yr} = \frac{1}{150}AC_{Ra} + \frac{1}{100}AC_{Th} + \frac{1}{1500}AC_{K} \quad (3.7)$$

where AC_{Ra}, $AC_{Th,}$ and AC_{k} are the average activity concentrations of ^{226}Ra, ^{232}Th and ^{40}K in rock samples respectively expressed in $Bqkg^{-1}$.

3.8.4 Radium equivalent (Ra_{eq})

It pertains to the collective activities of ^{226}Ra, ^{232}Th, and ^{40}K, which are presumed to produce an equivalent quantity of gamma dose rate as 1 $Bqkg^{-1}$ of ^{226}Ra, utilising the values of 0.7 $Bqkg^{-1}$ for ^{232}Th and 13 $Bqkg^{-1}$ for ^{40}K, as reported by (Amrani &

Tahtat, 2001). Equation (3.8) provides the methodology for calculating the radium equivalent, which is derived from an empirical correlation.

$$Ra_{eq} = AC_{Ra} + 1.423AC_{Th} + 0.077AC_{K} \quad (3.8)$$

Where the activity concentrations of ^{226}Ra, ^{232}Th, and ^{40}K in rock samples are expressed in Bqkg^{-1} as AC_{Ra}, AC_{Th} and AC_{K} respectively.

3.8.5 Absorbed Dose Rate (ADR)

The term "absorbed dose rate" pertains to the quantity of energy from radiation that is absorbed by a specific unit of mass. The statement pertains to the quantification of radiation exposure experienced by biological matter at a particular site, which is caused by either physical or chemical mechanisms. As per the findings of UNSCEAR, (2000), the calculation of the ADR is determined by taking into account the activity concentrations of ^{238}U (^{226}Ra), ^{232}Th and ^{40}K and utilising the conversion factors of activity concentration dose (nGy^{-1} per Bqkg^{-1}) which are 0.462 (0.427), 0.622 and 0.043 respectively. The dose rate was calculated using equation (3.9).

$$ADR = 0.427AC_{Ra} + 0.662AC_{Th} + 0.043AC_{K} \quad (3.9)$$

3.8.6 Annual Effective Dose Rate (AEDR)

The annual effective dose rate associated with radioactivity in rocks, which was relevant to the effective annual dose rate of the population, was calculated using a conversion factor of 0.7 SvGy^{-1} (UNSCEAR, 2000). The occupancy factors for the interior and exterior were 0.8 and 0.2 respectively. The computation of the yearly effective dosages for both indoor and outdoor settings was conducted utilising the equations (3.10) and (3.11) (UNSCEAR, 2000).

$$AEDR_{in} = ADR(nGyh^{-1}) \times 8760(hy^{-1}) \times 0.8 \times 0.7(SvGy^{-1}) \times 10^{-6} \quad (3.10)$$

$$AEDR_{out} = ADR(nGyh^{-1}) \times 8760(hy^{-1}) \times 0.2 \times 0.7(SvGy^{-1}) \times 10^{-6} \quad (3.11)$$

The variable $AEDR_{in}$ denotes the Annual Effective Dose received indoors, while the variable $AEDR_{out}$ denotes the Annual Effective Dose received outdoors. The total number of hours worked in a year is 8760 (UNSCEAR, 2000).

CHAPTER FOUR

RESULTS AND DISCUSSIONS

4.1 Introduction

This chapter presents the results and discussions for the radiological parameters below; radiation hazard indices, activity utilization index, annual effective and absorbed dose rate, and radium equivalent. The guidelines and conversion factors provided by (UNSCEAR, 2000) were utilized for this purpose.

4.2 Natural activity concentrations

Equation (3.4) was used to determine the amounts of ^{232}Th, ^{238}U and ^{40}K in the samples that were examined, and the findings are provided in Table A1 (Appendix IV). The study encompassed the computation of activity concentration of ^{232}Th, ^{238}U and ^{40}K in each sample, leading to the determination of the mean activity concentration for every excavation site. The investigation documented the average activity concentration of ^{232}Th, ^{238}U and ^{40}K to be 101 ± 5.08 Bq/kg, 56 ±2.81 Bq/kg and 1100 ± 55.03 Bq/kg with the ranges of 41 ± 2.07 to 138±6.91 Bq/kg, 26±1.34 to 116±5.8 Bq/kg and 256±12.82 to 1919±95.99 Bq/kg respectively.

The heterogeneity in the levels of activity concentrations detected among these quarries can be ascribed to the non-uniform dispersion of naturally occurring radioactive isotopes and geological variables. In addition to this, the amount of K-40 found in each of the analysed quarries was much greater than the number that is considered to be typical for the whole world. Eight of the quarries (Q2, Q6, Q7, Q8, Q10, Q11, Q13 and Q14) that were surveyed displayed activity concentrations of U-238 that were below the worldwide mean. Furthermore, it was observed that Q13 exhibited a lower activity concentration of Th-232, whereas Q12 recorded a value for K-40 that was below the worldwide mean. The minerals' presence may be attributed

to the relatively higher mean activity concentration of K-40 in comparison to that of Th-232 and U-238 (Table A1, Appendix IV).

According to Achola, (2009) findings, the elevated concentrations of primordial radionuclides detected in quarries could potentially be attributed to the buildup of radioactive substances within phosphate, quartzite, sandstone, and granite reserves. The findings indicate that the activity concentration of ^{40}K exhibited a consistent elevation compared to that of ^{226}Ra and ^{232}Th across all samples, a typical feature of crustal substances. The heightened concentrations of potassium were ascribed to the existence of minerals like orthoclase and biotite (Wanyama et al., 2020). Figure 4.1 illustrates the activity concentration of U-238, Th-232 and K-40 from Table A1, Appendix IV.

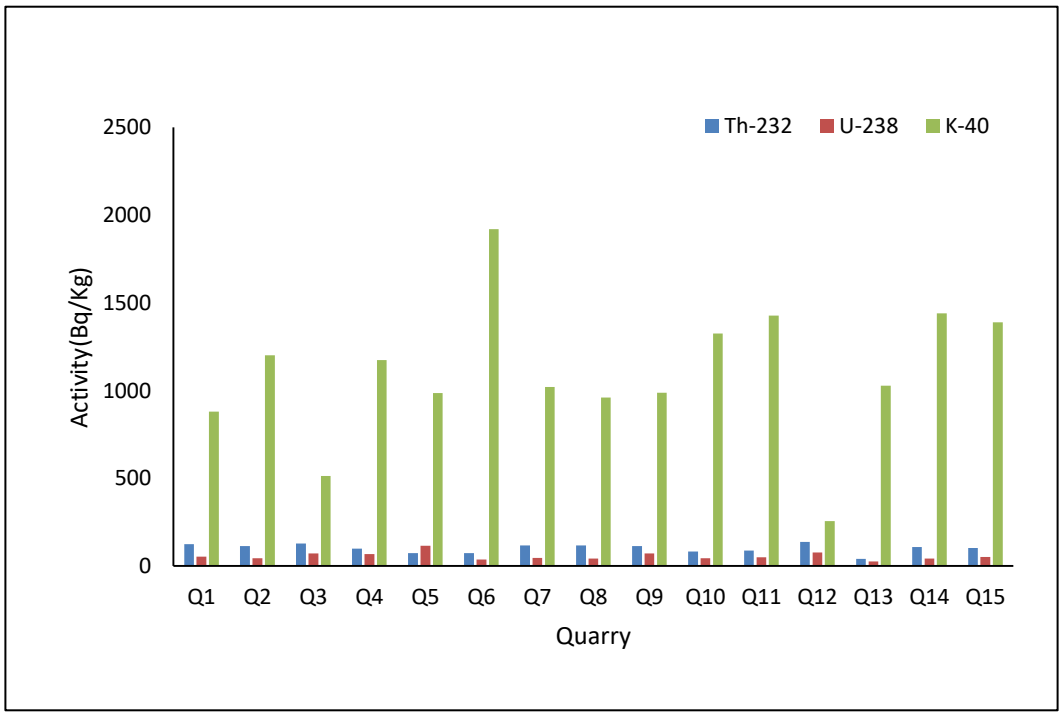

Figure 4.1: A bar graph displaying the activity concentration of ^{238}U, ^{232}Th and ^{40}K in rock samples

The findings indicate a considerable degree of diversity in the levels of activity concentrations of the examined radionuclides among the gathered rock specimens, which can be ascribed to the geological structures of the investigated region. According to the County Government of Kericho, (2023) Physiographic & Natural Resources report, the area of study is composed of metamorphic, igneous and volcanic rocks which may explain the detected fluctuations in activity concentrations.

A relatively even distribution of Thorium activity concentration was exhibited with the exception of a single quarry that recorded a lower value. Conversely, while the activity concentration of Uranium was generally low, it was observed to be fairly distributed throughout the region, with only a few instances of extreme values. This is because thorium is much more abundant than uranium and is enriched with acid igneous rocks (granites and monazite) which are resistant mineral and remain intact when rocks are weathering and are transported down the hill by water, wind and the gravity and accumulated there (Commonwealth of Australia (Geoscience Australia), 2021). Q12 registered a higher level of thorium due to it's geological position. The quarry is along the river therefore the elevated value was due to the presences of igneous rocks (granites) which are swept from up hill. The activity concentration of the three radionuclides has been observed to exhibit a normal distribution, as their values fall within the expected range of such a distribution (Kebwaro, 2009).

The levels of activity concentrations surpassed the threshold worldwide standards but remain below the permissible limits established for Th-232, U-238 and K-40, which are 1000 Bq/kg, 1000 Bq/kg and 100000 Bq/kg respectively. Therefore, it can be inferred that the rocks obtained from the quarries located in Kericho county are deemed suitable for utilization.

4.3 Radiation Hazard indices

The primary aim of the investigation was to assess the potential negative consequences related to exposure to high-energy emissions originating from Uranium-238 (^{238}U), Potassium-40 (^{40}K) and Thorium-232 (^{232}Th) found in rock samples collected from specific quarries in Kericho County. To carry out this evaluation, the researchers computed both the external and internal hazard indices, which serve as key indicators of radiation risk. The results of this comprehensive assessment are presented in Table A1, in Appendix IV. By analyzing these indices, the study seeks to provide a clearer understanding of the health implications associated with exposure to these radionuclides in the local environment.

4.3.1 External hazard index

Equation (3.5) was employed to calculate the external exposure resulting from gamma radiation. The findings revealed that the measured values varied between 0.4 ± 0.02 mSv/y and 0.8 ± 0.04 mSv/y, with the average exposure recorded at 0.8 ± 0.04 mSv/y. It is crucial to note that this average value is below the universally accepted threshold of 1 mSv/y, as established by the International Commission on Radiological Protection (ICRP, 2005). Consequently, it can be concluded that the rocks sourced from quarries in Kericho County do not pose any significant threat to the health and well-being of the local population. This assessment reinforces the safety of using these rocks in construction and other applications, ensuring that residents are not subjected to harmful levels of radiation exposure. Overall, the findings underscore the importance of ongoing monitoring to maintain safety standards in the region.

4.3.2 Internal hazard index

The internal exposure resulting from the inhalation and ingestion of the radionuclides was assessed using Equation (3.6). The results obtained through computation yielded

a range of values that spanned from 0.5 ± 0.02 mSv/y to 1.1 ± 0.05 mSv/y, with a mean value of 0.9 ± 0.04 mSv/y. The majority of the gathered samples exhibited measurements below the internationally suggested threshold, albeit a minority of the samples displayed marginally elevated values (Holm et al., 2006). The phenomenon under observation can be explained by the fact that the mean value of the indices obtained from the analyzed samples was found to be below the prescribed threshold Nevertheless, it is important to highlight that all recorded values were significantly lower than the threshold limit of 100 mSv/y established by the International Commission on Radiological Protection (ICRP, 2005). This finding suggests that the potential health hazards associated with the rocks are minimal and pose no significant risk to individuals. Additionally, Figure 4.2 illustrates graphical representations of both the internal and external hazard indices, as detailed in Table A2 of Appendix V. These visual representations further reinforce the study's conclusions regarding the safety of the rocks in relation to radiation exposure.of 1 unit, as per the guidelines established by ICRP (Table A2, Appendix V).

Figure 4.2: A graph illustrating the radiation hazard indices of the rock samples

4.4 Activity utilization index

Calculation of I_{yr} was done by employing equation (3.7). The obtained values ranged from 1.2 ± 0.06 to 2.3 ± 0.11 with an average activity index of 2.1 ± 0.10 as shown in Figure 4.3 and Table A2 (Appendix V).

When the utilization index is less than or equal to 2, it corresponds to an annual effective dose rate of 0.3 mSv. Conversely, when the utilization index is greater than 2 but less than 6, it corresponds to an annual effective dose rate of 1 mSv. This means that if the annual effective dose rates exceed the globally recommended value of 1 mSv, the activity index would necessarily be greater than 6. This relationship highlights the importance of monitoring the utilization index, as it provides valuable insight into radiation exposure levels and ensures that safety thresholds are maintained for those potentially exposed.(Achola, 2009).

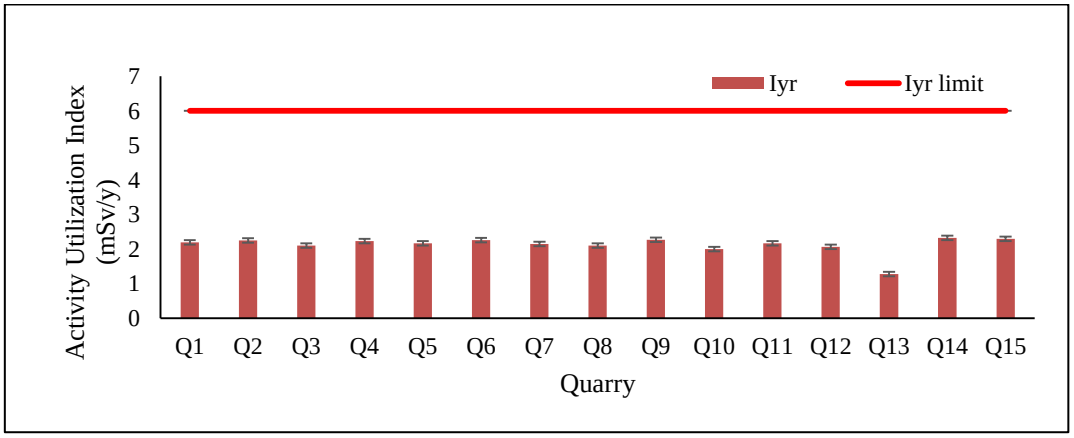

Figure 4.3: Graphical Representation of Activity Utilization Index of the Collected Quarry Samples

The mean activity utilization index recorded in the study was 2.1 ± 0.1, which is significantly below the maximum recommended value of 6 units as established by the International Commission on Radiological Protection (ICRP, 2000). Consequently,

individuals who regularly interact with the rock fragments are not at any substantial risk from radiation exposure, ensuring their safety

4.5 Radium equivalent (Ra_{eq})

The objective of the study assessed the potential health hazards associated with exposure to high-energy emissions emanating from ^{238}U, ^{232}Th, and ^{40}K present in rock samples obtained from Kericho County. The radium equivalent values were computed through utilization of equation (3.8) to address the inconsistent distribution of said elements in the rock samples and displayed in Table A2 (Appendix V). The obtained measurements exhibited a range of 165 ± 8.25 Bq/kg to 309 ± 15.47 Bq/kg and the average value was determined to be 285 ± 14.28 Bq/kg and shown in Figure 4.4. The observation's significance stems from the mean value's failure to meet the established threshold of 370 Bq/kg as specified by UNSCEAR, (2000). The findings suggest that the radium equivalent values of all quarries within the examined region were within the acceptable threshold. Therefore, the rocks procured from this region pose minimal threat to the well-being of the general populace.

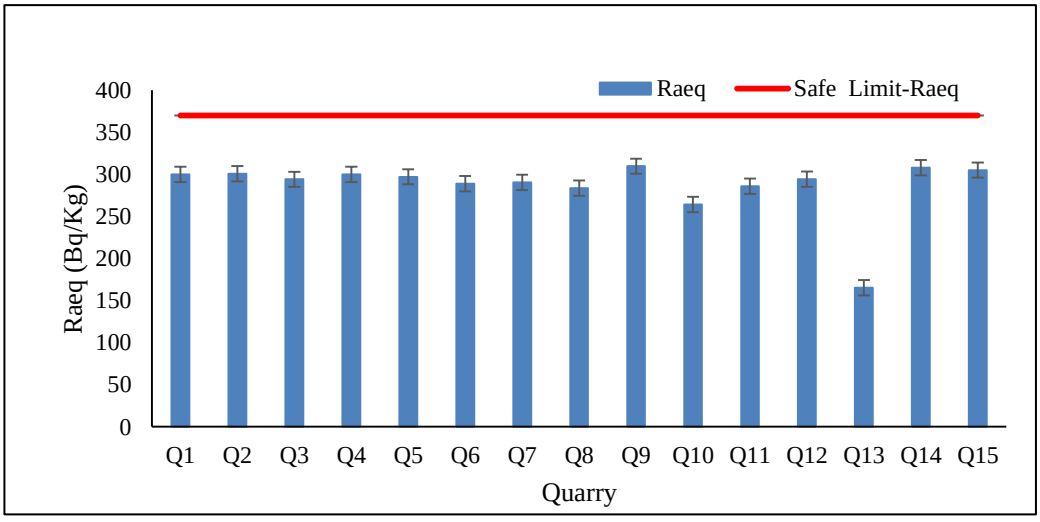

Figure 4.4: A bar grap showing the radium equivalent of rock samples

4.6 Dose rates

4.6.1 Absorbed dose rate

The computation was performed utilizing the equation (3.9) and recorded in Table A2 (Appendix V). The Annual Dose Rate (ADR) exhibited a range of values with the minimum being 83 ± 4.16 nGy/h and the maximum being 152 ± 7.6 nGy/h. The average value of ADR was calculated to be 138 ± 6.94 nGy/h. The observed ADR values were discovered to exceed the globally recommended threshold of 60 nGy/h, yet remained below the criterion limit of 1500 nGy/h, as stipulated by the (UNSCEAR, 2000). The dose rates for the quarries examined are presented in Figure 4.5.

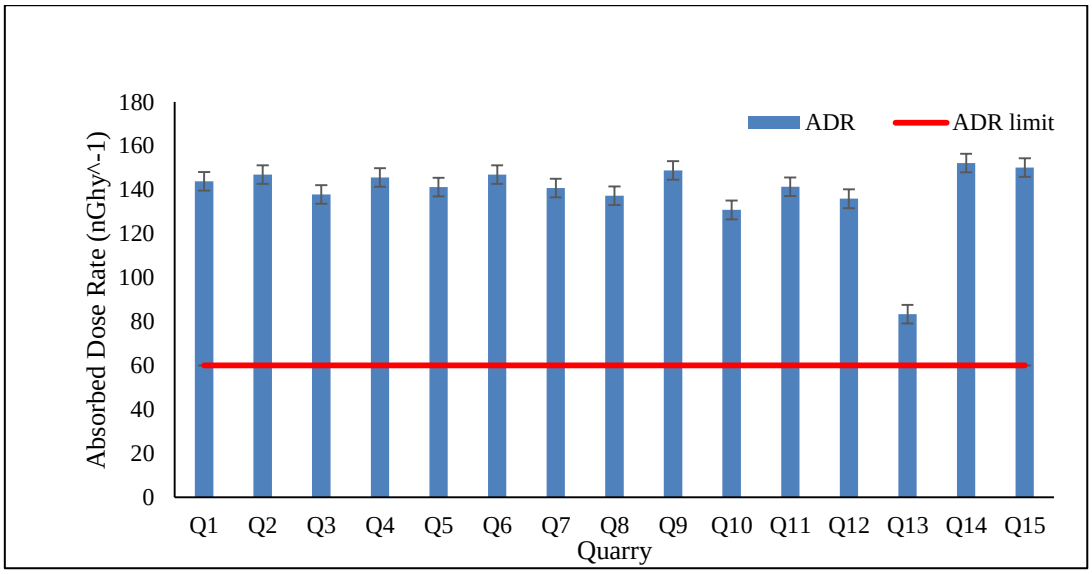

Figure 4.5: A graph for comparative analysis, depicting the absorbed dose rate of the collected samples

The observed samples displayed a dose rate of absorption that was higher than the global mean of 60 nGy/h. However, they were still below the exemption threshold of 1500 nGy/h, as established by (UNSCEAR, 2000). The elevated values observed in the investigated area can be attributed to the geological composition and uneven

distribution of primordial radioisotopes due to the existence of granitic and monazitic rocks that manifest an enrichment in Uranium-238, Thorium-232 and Potassium-40 within the igneous, volcanic, and metamorphic lithologies. Furthermore, computations were conducted to determine the yearly effective dose rates for both interior and exterior settings, alongside the absorbed dose rate.

4.6.2 Annual effective dose rates (AEDR)

Determination of AEDR was done using conversion factors as per UNSCEAR, (2000) which converts ADR to AEDR (namely: Indoor annual effective dose rate and Outdoor annual effective dose rate) which is used to gauge how hazardous the rocks are to the populace.

4.6.2.1 Indoor annual effective dose rate ($AEDR_{in}$)

The calculation of $AEDR_{in}$ was conducted using equation (3.10). The computed values were within the range of 0.4 ± 0.02 mSv/y to 0.7 ± 0.03 mSv/y, with an average of 0.6 ± 0.03 mSv/y, as shown in Table A2 (Appendix V). The observed variations in the indoor annual effective dose rates among the collected samples can be elucidated by the alterations in the activity concentration of each sample, as illustrated in Figure 4.6.

The study found that the indoor dose rates in all assessed quarries were within the globally recommended threshold of 1 mSv/y. This finding indicates that the levels of radiation exposure associated with these rocks are deemed safe for use, supporting their application in various construction activities without posing significant health risks

4.6.2.2 Outdoor annual effective dose rate ($AEDR_{out}$)

The calculation of $AEDR_{out}$ was performed using equation (3.11), with values ranging from 0.1 ± 0 mSv/y to 0.1 ± 0 mSv/y, and an average value of 0.1 ± 0 mSv/y, as displayed in Table A2 (Appendix V). The study determined that the effective dose values for outdoor exposure were below the acceptable limit as recommended by the appropriate regulatory bodies. Each sample exhibited a measurement of 0.1 ± 0 mSv/y as shown in Figure 4.6. Based on the findings of the study, it can be concluded that the rocks located in the region do not pose a noteworthy radiological hazard to the populace, as the yearly effective dose rate assessments were lower than the global average of 1 mSv/y.

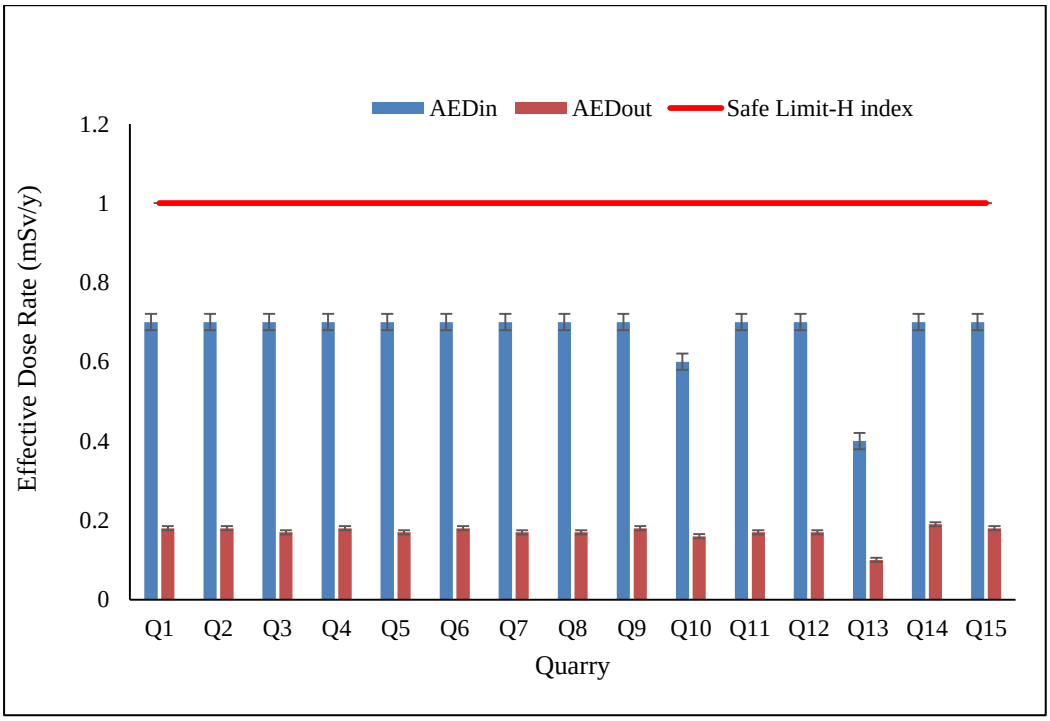

Figure 4.6: A graphical representation in the form of a bar chart depicting the yearly effective dose rate of the collected samples

CHAPTER FIVE

SUMMARY, CONCLUSIONS AND RECOMMENDATIONS

5.1 Introduction

This chapter summarizes the results obtained from the analysis of the natural radioactivity levels of rocks excavated from the selected Kericho County quarries and the recommendations on future radiological surveys

5.2 Summary of findings

This study utilized a sodium iodide (NaI(TI)) gamma-ray spectrometer to assess the levels of natural radioactivity present in rock samples collected from quarries in Kericho County, a region where these rocks are commonly used for construction purposes. The primary objective of the investigation was to evaluate the potential risks associated with these rocks for individuals who frequently come into contact with rock fragments during construction activities or while living nearby. By measuring the radioactivity levels, the study aimed to identify any health hazards that could arise from exposure to these materials, ensuring that safety measures are in place to protect the community and workers in the area.

This investigation provides detailed findings on the average activity concentrations of Thorium-232 (^{232}Th), Uranium-238 (^{238}U), and Potassium-40 (^{40}K) in rock specimens obtained from specific quarries. The documented average activity concentrations were 101 ± 5.08 Bq/kg for 232Th, 56 ± 2.81 Bq/kg for 238U, and 1100 ± 55.03 Bq/kg for 40K. These results indicate that while the mean levels of activity concentrations conform to the permissible thresholds established for safety, they exceed the recommended global benchmarks. This discrepancy highlights the need for ongoing

monitoring and assessment to ensure that the radiation levels remain within acceptable limits, thereby safeguarding public health and environmental safety.

The investigation revealed that the average measurement of the external hazard index was 0.8 ± 0.04 mSv/y, while for the internal hazard index was found to be 0.9 ± 0.04 mSv/y. Both of these values fall well within the permissible limit of 1 mSv/y, indicating a relatively low risk associated with external and internal radiation exposure from the rock samples. Additionally, the mean activity utilization index was recorded at 2.1 ± 0.1 mSv/y, which is significantly below the recommended threshold of 6 mSv/y. This finding further suggests that the materials from these quarries are safe for use in construction and other applications.

Moreover, the study determined that the average radium equivalent concentration in the selected quarries located in Kericho County was 285 ± 14.28 Bq/kg. Importantly, this value does not exceed the permissible limit of 370 Bq/kg, reinforcing the conclusion that the levels of natural radioactivity in these rocks are within acceptable safety standards. Overall, these findings highlight the importance of ongoing monitoring and assessment to ensure that radiation levels remain safe for human health and the environment, particularly in areas where these materials are used

The investigation revealed that the absorbed dose rate was measured at 138 ± 6.94 nGy/h, which surpasses the globally recommended threshold of 60 nGy/h. However, it still remains well within the acceptable maximum threshold limit of 1500 nGy/h, indicating that while the levels are elevated compared to the recommended guidelines, they do not pose an immediate risk.

Furthermore, the research results showed that the mean yearly effective dose rates for indoor environments were recorded at 0.6 ± 0.03 mSv/y, while for outdoor settings, the mean was 0.1 ± 0 mSv/y. Both of these values are significantly below the universally recognized threshold of 1 mSv/y, suggesting that exposure to radiation in these environments is within safe limits. This emphasizes the importance of ongoing monitoring to ensure that even elevated dose rates do not lead to health risks for individuals living and working in proximity to the studied areas

5.3 Conclusions

From the research findings the internal and external hazard indices were within the required radioactivity specification limits of one unit, excavation of rocks from the selected quarries of Kericho County provide minimal radioactive health risks to the inhabitants. As a result the health burden caused by natural background radiation from the excavated rocks on the population of this research area is within permitted limits, posing no substantial health risks. It can therefore be concluded that;

i) The findings indicate that the level of radiation exposure experienced by individuals who regularly handle rocks is negligible, resulting in a lower risk of developing cancer-related diseases. This conclusion suggests that the rocks sourced from Kericho County are safe for use in the construction of both residential and commercial buildings. Given that the radiation levels are within acceptable limits, stakeholders can confidently utilize these materials without significant concern for health risks. Therefore, the study supports the continued use of Kericho County rocks in construction projects, ensuring safety for both workers and future occupants of the structures built with these materials.

ii) The findings reported in this study will provide a crucial baseline representation of the background levels of radioactivity in the selected quarries and their surrounding environments. This data will serve as an important benchmark for evaluating any future changes in radioactive ambient levels that could result from geological activities or excavation operations. By establishing this foundational understanding, the study aims to facilitate more effective monitoring and assessment of potential risks over time. Furthermore, disseminating this information will help raise awareness about radiation risks, thereby informing decision-making processes at both county and national levels. This heightened awareness is essential for guiding policies related to the implementation and achievement of affordable housing, universal healthcare, and sustainable manufacturing practices. Ultimately, the insights gained from this research will support efforts to ensure public safety while promoting responsible development within the region.

iii) Mining in the quarries will generate job opportunities in a safer environment, contributing to the development of various industries. This growth will not only create employment but also attract investors looking to capitalize on the region's resources. As more businesses establish themselves in Kericho County, the local economy will experience a significant boost, leading to increased financial stability and growth for the community. Additionally, the overall economic progress will benefit the country at large, as a thriving local economy contributes to national development. This cycle of investment and job creation will ultimately enhance the quality of life for residents

5.4 Recommendations

Based on the first objective concerning the activity concentration of Potassium-40, Thorium-232, and Uranium-238, it is strongly recommended that continuous routine monitoring and effective management practices be implemented. This ongoing surveillance is crucial for maintaining safety and for the early detection of any potential increases or anomalies in the radiation levels. By regularly assessing these radionuclide concentrations, stakeholders can ensure that the levels remain within established safety limits. Proactive management will help mitigate any health risks associated with elevated radiation exposure and contribute to the overall well-being of the community and environment.

From the second objective related to the utilization index, radium equivalent, and radiological hazard indices (both external and internal), it is essential to implement continuous periodic checks. These regular assessments are necessary to ensure that the radiation levels remain within established safe limits. Additionally, this approach allows for the ongoing evaluation of any changes in these indices over time. By conducting routine monitoring, any gradual increases or concerning trends can be promptly detected and addressed. This proactive strategy will help to safeguard public health and mitigate potential risks associated with radiological exposure in the environment

Based on the third objective focusing on absorbed dose rate and annual effective dose rate (both indoor and outdoor) it is imperative to establish a monitoring system. This system should be designed to ensure that the radiation levels consistently remain below the established safe limits. Regular monitoring will also allow for the identification and assessment of any potential environmental changes that could

impact these dose rates. By maintaining vigilance in monitoring, it becomes possible to address any emerging issues swiftly and effectively, thereby protecting public health and ensuring a safe living environment for the community

In general, regular monitoring should be conducted even when radiation levels are low or within established safe limits, as this practice facilitates the early detection of any potential issues that may arise. Maintaining a consistent monitoring schedule allows for proactive management of radiological safety. Additionally, it is essential to keep detailed records of all measurements and observed trends, as this documentation will aid in identifying any unusual patterns or changes over time. Such comprehensive data collection is crucial for ensuring ongoing safety and for informing any necessary interventions or adjustments to monitoring protocols in the future.

5.5 Suggestions for further research

The research was conducted during a period characterized by low precipitation, which may have influenced the results. This limitation underscores the necessity for further investigations to be carried out across different seasons to obtain a more comprehensive understanding of how seasonal variations affect the findings. By examining the data throughout varying climatic conditions, researchers can achieve more reliable and uniform outcomes. This approach will enhance the robustness of the study and ensure that any conclusions drawn about the impact of seasonal changes on the parameters being measured are valid and applicable across different environmental contexts

The study did not account for the evaluation of several important metrics that are associated with the rocks collected from the research site. These metrics are crucial for a comprehensive understanding of the radiological implications of the materials

under investigation. Among the key radiological parameters that were overlooked are the annual gonadal equivalent dose, which indicates the potential radiation exposure to the reproductive organs over a year, and the representative gamma index, a measure that assesses the overall radiological hazard posed by gamma radiation.

Additionally, the study failed to consider the surplus cancer risk, which quantifies the increased likelihood of cancer development as a result of radiation exposure. This metric is particularly significant for assessing long-term health outcomes associated with living near or utilizing radioactive materials. Furthermore, the cumulative effective dose was not evaluated; this parameter reflects the total radiation exposure accumulated over time, which is essential for understanding potential health impacts. The cumulative health detriment, which encompasses the overall health effects of radiation exposure, was also not included in the study. Including these parameters would provide a more holistic assessment of the radiological safety and potential health risks associated with the rocks from the study location

This investigation did not address the potential presence of radon in the underground water sources located near the quarries where rock mining occurs. Radon is a naturally occurring radioactive gas that can accumulate in confined spaces, particularly in areas with geological formations that contain uranium or thorium. Given its health risks, including the potential to cause lung cancer with prolonged exposure, it is essential to evaluate the radon levels in the subterranean water reservoirs adjacent to the quarries currently being examined.

Determining the levels of Radon-222 in these water sources is critical, as it can help assess any potential health risks to individuals who might consume or come into contact with the water. Additionally, understanding the concentration of radon in the

water can inform local authorities and the community about safety measures that may need to be implemented. If significant levels of radon are detected, it may prompt further investigations or remediation efforts to mitigate exposure risks. Overall, including radon assessment in future studies would provide a more comprehensive evaluation of the radiological hazards associated with the quarries and ensure the safety of those living and working in the vicinity.

REFERENCES

Achola, S. O. (2009). *Radioactivity and elemental analysis of carbonatite rocks from Gwasi area, South Western Kenya* (Doctoral dissertation, University of NAIROBI).

Ahmed, A. A., & Hussein, M. I. (2011). Natural radioactivity measurements of basalt rocks in Sidakan district northeastern of Kurdistan region-Iraq. *International Journal of Geological and Environmental Engineering*, *5*(2), 66-73.

Amrani, D., & Tahtat, M. (2001). Natural radioactivity in Algerian building materials. *Applied Radiation and isotopes*, *54*(4), 687-689.

AS-Subaihi, F. A., Harb, S., & Abdullah, T. Natural Radioactivity Measurements of Basalt Rocks in Wadi Khuda Area, Southwest of Safaga, Eastern Desert of Egypt. *The International Journal of Engineering and Science (IJES)*, volume 8

Bachama, Y. D., Ahmed, A. L., Lawal, K. M., & Arabi, A. S. (2017). Natural Gamma Radiation in Rocks from Kerri-Kerri Formation, Northeastern Nigeria. *Journal of African Earth Sciences*, *130*, 269-273.

Commonwealth of Australia (Geoscience Australia). (2021). *Uranium and thorium*. Retrieved on 22nd July 2021 from https://www.ga.gov.au/education/classroom-resources/minerals-energy/australian-energy-facts/uranium-and-thorium

County Government of Kericho. (2023). *Physiographic & Natural Resources* Https://www.kericho.go.ke/location-position-and-size Retrieved 9th Aug 2021. (n.d.).retrieved on 22nd July 2021

Faanu, A., Adukpo, O. K., Tettey-Larbi, L., Lawluvi, H., Kpeglo, D. O., Darko, E. O., ... & Agyeman, L. (2016). Natural radioactivity levels in soils, rocks and water

at a mining concession of Perseus gold mine and surrounding towns in Central Region of Ghana. *SpringerPlus, 5*, 1-16.

Harb, S., El-Kamel, A. H., Zahran, A. M., Abbady, A., & Ahmed, F. A. (2014). Natural radioactivity measurements of basalt rocks in aden governorate, south of Yemen on Gulf of Aden. *Journal of Applied Physics*, *5*(6), 39-48.

Holm, L. E., COX, R., & VALENTIN, J. (2006). The 2006 recommendations of the international commission on radiological protection. *ICRP Publication*, *103*, 2007-03.

IAEA. (2004). *International Atomic Energy Agency, Soil sampling for environmental contaminants*, IAEA-TECDOC-1415 IAEA: Vienna, Austria.

IAEA. (2005). *International Atomic Energy Agency, Guidelines for radioelement mapping using gamma-ray spectrometry data,* Viena, Austria. pp 295.

ICRP. (2005). *Low-dose extrapolation of radiation related cancer risks*. International Commission on radiological protection. Oxford: Pentagon press. Annals of the ICRP, *35*(4), 1-140.

ICRP. (2000). *Protection of the public in situations of prolonged radiation exposure* ICRP Publication 82; Ann. ICRP 29 (1–2), Pentagon Press, Oxford.

Independent Electoral and Boundaries Commission, IEBC. (2013). *Map of Kenya and Kericho county*. Retrieved from https://www.google. com/ immigrationusa.us, on 9th Aug 2021

Kaniu, M. I., Angeyo, H. K., Darby, I. G., & Muia, L. M. (2018). Rapid in-situ radiometric assessment of the Mrima-Karuku high background radiation anomaly complex of Kenya. *Journal of environmental radioactivity, 188* , 47-57.

Kebwaro, J. M., Rathore, I. V. S., Hashim, N. O., & Mustapha, A. O. (2011). Radiometric assessment of natural radioactivity levels around Mrima Hill, Kenya. International *Journal of the physical sciences. 6*(13)*:*3105-3110.

Kebwaro, M. (2009). *Gamma ray spectrometry analysis of the surface soil around Mrima hill Kenya using NaI (Tl) detector and decomposition technique*. MSc. Thesis, Kenyatta University, Nairobi, Kenya.

Kenya Cancer Policy (KCP), 2019; https://www.Cancer.Org/Cancer/Cancer-Causes/Radiation- Exposure/Radon Retrieved on 18th Sep 2021 1233 Hrs., n.d

Khan, I. U., Qin, Z., Xie, T., Bin, z., Li, H., Sun, W., & Lewis, E. (2020). Evaluation of health hazards from radionuclides in soil and rocks of North Waziristan, Pakistan. *International Journal of Radiation Research, 18*(2), 243–253.

Kinyua, R., Atambo, V. O., & Ongeri, R. M. (2011). Activity concentrations of ^{40}K, ^{232}Th, ^{226}Ra and radiation exposure levels in the Tabaka soapstone quarries of the Kisii Region, Kenya. *African journal of environmental science and Technology, 5*(9), 682- 688.

Kipngeno, R. C. (2015). *Gamma-Ray Spectroscopic Analysis of Soil and Green Te a Leaves of Kericho County* (Doctoral dissertation, MSc. Thesis, Kenyatta University).20.

Kiprono, V. (2020). *Radiometric assessment of natural radioactivity levels and radiation hazard indices for soil samples in Kericho County, Kenya* (Doctoral dissertation, Kenyatta University).

Matsitsi, S. M., Linturi, J. M., Kebwaro, J. M., & Maweu, O. M. (2019). Effects of Seasonal Change on the Levels of Geogenic Radionuclides in Sand and Rocks

from Tyaa River deposit in Kitui County: Geophysics. *International Journal of Fundamental Physical Science, 9*(1), 14-19.

Mohanty, A. K., Sengupta, D., Das, S. K., Vijayan, V., & Saha, S. K. (2004). Natural radioactivity in the newly discovered high background radiation area on the eastern coast of Orissa, India. *Radiation measurements, 38*(2), 153-165.

Mulwa, B. M., Maina, D. M., & Patel, J. P. (2013). Radiological analysis of suitability of Kitui South limestone for use as building material. *International Journal of Fundamental Physical Sciences (IJFPS), 3*(2), 32-35.

Odumo, O. B., Mustapha, A. O., Patel, J. P., & Angeyo, H. K. (2011). Radiological survey and assessment of associated activity concentration of the naturally occurring radioactive materials (NORM) in the Migori artisanal gold mining belt of southern Nyanza, Kenya. *Applied Radiation and isotopes, 69*(6), 912-916.

Onjefu, S., Kamunda, C., & Abah, J. (2021). Health Risk Assessment of Natural Radioactivity in Wasteland Soils in Okakarara, Namibia. *Arab Journal of Nuclear Sciences and Applications, 54*(2), 143–150.

Pavan, M. V. R., & Andrew, R. B. (2020). *Principles of Gamma Ray Spectroscopy and Applications in Nuclear Forensics* https://chem.libretexts.org.

Ragheb, M. (2011). *Gamma Rays Interactions with Matter. Nuclear, Plasma and Radiation Science.* Inventing the Future," https://netfiles. Uiuc. Edu. Retrived on 9th Aug 2021

Rasmussen, J. O., & Ellis, P. (2023). *Radioactivity*. Encyclopedia Britannica. Retrived on 9th Aug 2021 from https://www.britannica.com/science/radioactivity

Rich, J. N. (2007). Cancer stem cells in radiation resistance. *Cancer research*, *67*(19), 8980- 8984.

Risica, S., & Nuccetelli, C. (2001). Building materials as a source of population exposure to ionizing radiation. *Physica medica*, *17*(1), 3-8.

Rosianna, I., Nugraha, E. D., Syaeful, H., Putra, S., Hosoda, M., Akata, N., & Tokonami, S. (2020). Natural Radioactivity of Laterite and Volcanic Rock Sample for Radioactive Mineral Exploration in Mamuju, *Indonesia. Geosciences*, *10*(9), 376.

Sangura, M. T., & Waswa, N. M. (2012). *Gamma-Ray Spectrometric Determination And Multivariate Analysis Of Radionuclide Fluxes In Shore Sediment At Port Victoria, Kenya.*

Seuntjens, J. P., Strydom, W. Y. N. A. N. D., & Shortt, K. R. (2005). *Dosimetric principles, quantities and units. Radiation oncology physics*: A handbook for teachers and students. PodgorsakEB,editor.Vienna,Austria:IAEA. https://inis.iaea.org.

Sindani, L., Waswa, M. N., Maingi, F., & Wanyama, C. K. (2022). Measurement of radiological parameters in harvested sand in Bungoma county rivers, Kenya. *ITEGAM-JETIA*, *8*(33), 21–25.

Singh, S., Rani, A., & Mahajan, R. K. (2005). ^{226}Ra, ^{232}Th and ^{40}K analysis in soil samples from some areas of Punjab and Himachal Pradesh, India using gamma ray spectrometry. *Radiation Measurements*, *39*(4), 431–439.

Syaeful, H., Sukadana, I. G., & Sumaryanto, A. (2014). Radiometric mapping for naturally occurring radioactive materials (NORM) assessment in Mamuju, West Sulawesi. *Atom Indonesia, 40*(1), 33-39.

Tsai, T. L., Lin, C. C., Wang, T. W., & Chu, T. C. (2008). Radioactivity concentrations and dose assessment for soil samples around nuclear power plant IV in Taiwan. *Journal of radiological protection, 28*(3), 347.

Turyahabwa, E. S., Jurua, E., Oriada, R., Mugaiga, A., & Enjiku, D. B. (2016). Determination of natural radioactivity levels due to mine tailings from selected mines in Southwestern Uganda. *International Journal of Geological and Environmental Engineering., 6*, 154-163.

Tzortzis, M., Svoukis, E., & Tsertos, H. (2004). A comprehensive study of natural gamma radioactivity levels and associated dose rates from surface soils in Cyprus. *Radiation Protection Dosimetry, 109* (3), 214-224.

UNSCEAR, S. (2000). United Nations Scientific Committee on the Effects of Atomic Radiation. *Sources and effects of ionizing radiation*. Report to the General Assembly, with Scientific Annexes United Nations, New York.

Uosif, M. (2011). Specific activity of ^{226}Ra, ^{232}Th and ^{40}K for assessment of radiation hazards from building materials commonly used in Upper Egypt. Süleyman Demirel *Üniversitesi Fen Edebiyat Fakültesi Fen Dergisi, 6*(2), 120-126.

Wanyama, C. K., Masinde, F. W., Makokha, J. W., & Matsitsi, S. M. (2020). Estimation of radiological hazards due to natural radionuclides from the Rosterman gold mine tailings, Lurambi, Kakamega, Kenya. *Radiation Protection Dosimetry, 190*(3), 324- 330

APPENDICES

Appendix I: NACOSTI Licence Certificate.

REPUBLIC OF KENYA

NATIONAL COMMISSION FOR SCIENCE,TECHNOLOGY & INNOVATION

Ref No: 203135

Date of Issue: 02/June/2022

RESEARCH LICENSE

This is to Certify that Ms.. BETTY CHEPNGETICH of University of Kabianga, has been licensed to conduct research in Kericho on the topic: GAMMA-RAY SPECTROMETRIC ANALYSIS OF ROCKS USED FOR CONSTRUCTION FROM SELECTED QUARRIES IN KERICHO COUNTY, KENYA for the period ending : 02/June/2023.

License No: NACOSTI/P/22/17998

203135

Applicant Identification Number

Director General
NATIONAL COMMISSION FOR SCIENCE,TECHNOLOGY & INNOVATION

Verification QR Code

NOTE: This is a computer generated License. To verify the authenticity of this document, Scan the QR Code using QR scanner application.

Figure A 1: Licence Certificate from National Commission for Science, Technology, and Innovation**.**

Appendix II: BGS Approval letter

UNIVERSITY OF KABIANGA
ISO 9001:2015 CERTIFIED
OFFICE OF THE DIRECTOR, BOARD OF GRADUATE STUDIES

REF: PGC/PHY/005/19 **DATE: 16TH MAY, 2022**

Betty Chepngetich,
MAPS,
University of Kabianga,
P.O Box 2030- 20200,
KERICHO.

Dear Ms. Chepngetich,

RE: CLEARANCE TO COMMENCE FIELD WORK

I am glad to inform you that the Board of Graduate Studies during its meeting on 12th January 2022 approved your research proposal entitled " **Gamma-Ray Spectrometric Analysis of rocks used for Construction from Selected Quarries in Kerichio county, Kenya ".**

I am also acknowledging receipt of your corrected proposal via email and hard copies. You are now free to commence your field work on condition that you obtain a research permit from NACOSTI.

Please note that, you are expected to publish at least one (1) paper in a peer reviewed journal before final examination (oral defense) of your Masters thesis.

Thank you.

Yours Sincerely,

16 MAY 2022

Prof. J. K. Kibett
DIRECTOR, BOARD OF GRADUATE STUDIES.

cc 1. Dean, SST
2. HOD, MAPS
3. Supervisors

Figure A 2: Letter of clearance to commence field work from University of Kabianga

Appendix III: Collection, Preparation, Placement of sample, and Formation of spectrum and Analysis

Figure A 3

Collection of Samples

Figure A 4

Preparation of samples

Figure A 5

Placement of Samples in the Spectrometer

Figure A 6

Formation of spectrums and Analysis

Appendix IV: Activity Concentrations and Radiation Hazard Indices

Table A 1: Activity Concentrations (AC of Th-232, U-238 and K-40) and Radiation Hazard Indices (H_{ex} and H_{in}) of the Collected Samples

QUARRY	AC Th-232 Bq/Kg	AC U-238 Bq/Kg	AC K-40 Bq/Kg	H_{ex} mSv/y	H_{in} mSv/y
Q1	125±6.26	53±2.68	880±44.01	0.8±0.04	0.9±0.04
Q2	114±5.73	45±2.25	1201±60.08	0.8±0.04	0.9±0.04
Q3	128±6.43	71±3.56	512±25.62	0.8±0.04	1.0±0.05
Q4	99±4.98	67±3.38	1174±58.74	0.8±0.04	1.0±0.05
Q5	73±3.69	116±5.8	985±49.28	0.8±0.04	1.1±0.05
Q6	72±3.64	37±1.85	1919±95.99	0.8±0.04	0.9±0.04
Q7	116±5.83	45±2.28	1020±51.01	0.8±0.04	0.9±0.04
Q8	116±5.83	43±2.16	961±48.06	0.7±0.03	0.9±0.04
Q9	113±5.67	72±3.60	987±49.37	0.8±0.04	1.0±0.05
Q10	82±4.12	44±2.22	1325±66.25	0.7±0.03	0.8±0.04
Q11	88±4.44	49±2.46	1427±71.37	0.8±0.04	0.9±0.04
Q12	138±6.91	77±3.88	256±12.82	0.8±0.04	1.0±0.05
Q13	41±2.07	26±1.34	1027±51.38	0.4±0.02	0.5±0.02
Q14	108±5.40	43±2.16	1439±71.98	0.8±0.04	0.9±0.04
Q15	103±5.15	51±2.57	1388±69.42	0.8±0.04	1.0±0.05
MIN	**41±2.07**	**26±1.34**	**256±12.82**	**0.4±0.02**	**0.5±0.02**
MAX	**138±6.91**	**116±5.80**	**1919±95.99**	**0.8±0.04**	**1.1±0.05**
AVERAGE	**101±5.08**	**56±2.81**	**1100±55.03**	**0.8±0.04**	**0.9±0.04**

Appendix V: Activity Utilization Index, Radium Equivalent , Absorbed Dose Rate and Annual Effective Dose Rates

Table A 2: The activity Utilization Index (I_{yr}), Radium Equivalent (Ra_{eq}), Absorbed Dose Rate (ADR) and Annual Effective Dose Rates ($AEDR_{in}$ and $AEDR_{out}$) pertaining to the collected rock samples

QUARRY	I_{yr} mSv/y	Ra_{eq} Bq/Kg	ADR nGy/h	$AEDR_{in}$ mSv/y	$AEDR_{out}$ mSv/y
Q1	2.1±0.10	299±14.99	143±7.19	0.7±0.03	0.1±0
Q2	2.2±0.11	300±15.03	146±7.34	0.7±0.03	0.1±0
Q3	2.1±0.10	293±14.69	137±6.89	0.6±0.03	0.1±0
Q4	2.2±0.11	299±14.99	145±7.28	0.7±0.03	0.1±0
Q5	2.1±0.10	297±14.85	141±7.05	0.6±0.03	0.1±0
Q6	2.2±0.11	288±14.44	146±7.34	0.7±0.03	0.1±0
Q7	2.1±0.10	290±14.51	140±7.03	0.6±0.03	0.1±0
Q8	2.0±0.10	283±14.17	137±6.86	0.6±0.03	0.1±0
Q9	2.2±0.11	309±15.47	148±7.42	0.7±0.03	0.1±0
Q10	2.0±0.10	263±13.19	130±6.53	0.6±0.03	0.1±0
Q11	2.1±0.10	285±14.28	141±7.07	0.6±0.03	0.1±0
Q12	2.0±0.10	294±14.70	135±6.79	0.6±0.03	0.1±0
Q13	1.2±0.06	165±8.25	83±4.16	0.4±0.02	0.1±0
Q14	2.3±0.11	307±15.39	152±7.60	0.7±0.03	0.1±0
Q15	2.2±0.11	305±15.25	150±7.50	0.7±0.03	0.1±0
MIN	**1.2±0.06**	**165±8.25**	**83±4.16**	**0.4±0.02**	**0.1±0**
MAX	**2.3±0.11**	**309±15.47**	**152±7.60**	**0.7±0.03**	**0.1±0**
AVERAGE	**2.1±0.10**	**285±14.28**	**138±6.94**	**0.6±0.03**	**0.1±0**

Appendix VI: Decay Chain of ^{238}U and ^{232}Th Radionuclides

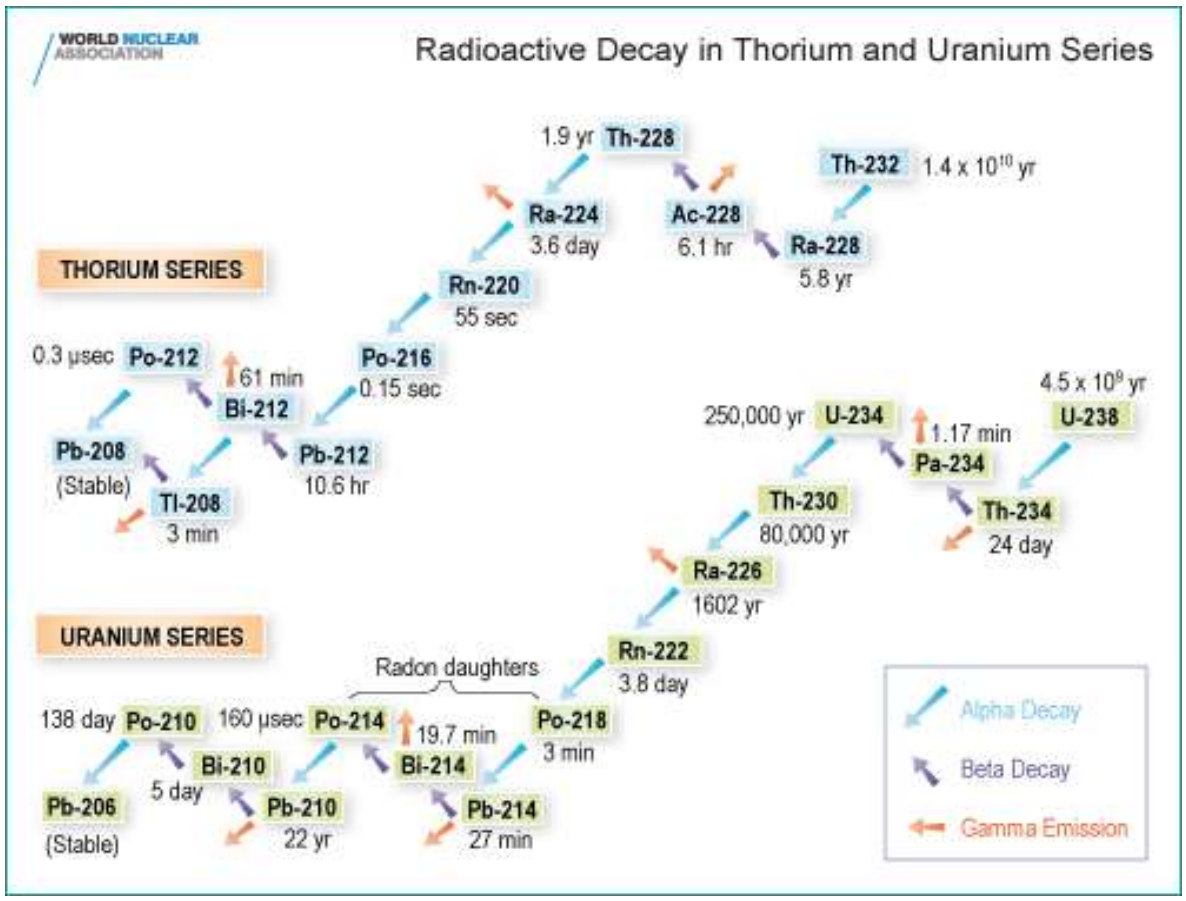

Figure A 7: Decay chain of ^{238}U and ^{232}Th radionuclides (Wanyama et al., 2020)

Appendix VII: Publication and Conference Papers' Titles

Publication

1.Betty, C., Masinde, F. W., Rotich, E. K., & Wanyama, C. K. (2022). Radiological hazard levels of construction rocks excavated from quarries in Kericho county, Kenya. *ITEGAM-JETIA*, *8*(37), 28-32.

Conferences

2. Betty, C., Masinde, F. W., & Rotich, E. K., (2023). Natural Radioactivity Levels in Rocks Excavated from Kericho County Quarries, Kenya. 3rd University of Kabianga multidisciplinary conference, 27th-28th Sept 2023.

3. Betty, C., Masinde, F. W., Rotich, E. K., & Wanyama, C. K. (2022). Radiological hazard levels of construction rocks in Kericho county, Kenya. 2nd Bomet University College international conference, 29th-30th Nov 2022

Appendix VIII: Antiplagiarism Report

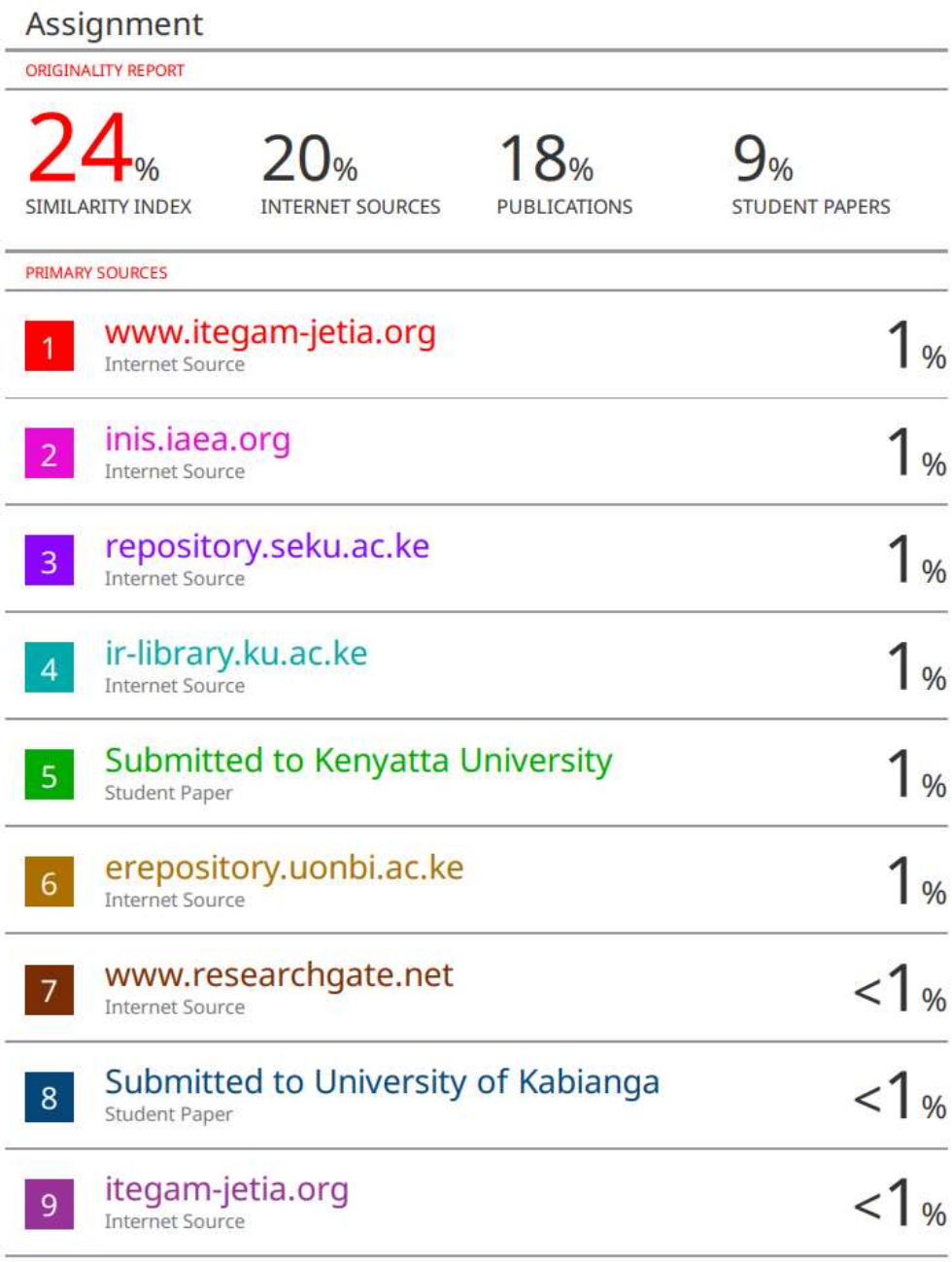

Assignment

ORIGINALITY REPORT

24%	20%	18%	9%
SIMILARITY INDEX	INTERNET SOURCES	PUBLICATIONS	STUDENT PAPERS

PRIMARY SOURCES

1	www.itegam-jetia.org Internet Source	1%
2	inis.iaea.org Internet Source	1%
3	repository.seku.ac.ke Internet Source	1%
4	ir-library.ku.ac.ke Internet Source	1%
5	Submitted to Kenyatta University Student Paper	1%
6	erepository.uonbi.ac.ke Internet Source	1%
7	www.researchgate.net Internet Source	<1%
8	Submitted to University of Kabianga Student Paper	<1%
9	itegam-jetia.org Internet Source	<1%

Figure A 8: Antiplagiarism Report